Final Scientific/Technical Report

Project Title: Establishment of a Laboratory for Biofuels Research at the University of Kentucky

Principal Investigator: Rodney Andrews

Type of Report: Final Scientific/Technical Report

Reporting Period Start Date: September 1, 2008

Reporting Period End Date: December 31, 2012

Written by: Mark Crocker (co-PI) and Czarena Crofcheck (co-PI)

Date of Report: March 29, 2013

Award Number: DE-FG36-08GO88043

Recipient: University of Kentucky Research Foundation

Project Location: Center for Applied Energy Research, University of Kentucky
2540 Research Park Dr., Lexington, KY 40511

Disclaimer

Abstract

This project was aimed at the development of the biofuels industry in Kentucky by establishing a laboratory to develop improved processes for biomass utilization. The facility is based at the University of Kentucky Center for Applied Energy Research and the Department of Biosystems and Agricultural Engineering, and constitutes an “open” laboratory, i.e., its equipment is available to other Kentucky researchers working in the area. The development of this biofuels facility represents a significant expansion of research infrastructure, and will provide a lasting resource for biobased research endeavors at the University of Kentucky. In order to enhance the laboratory’s capabilities and contribute to on-going biofuels research at the University of Kentucky, initial research at the laboratory has focused on the following technical areas: (i) the identification of algae strains suitable for oil production, utilizing flue gas from coal-fired power plants as a source of CO_2; (ii) the conversion of algae to biofuels; and (iii) the development of methods for the analysis of lignin and its deconstruction products. Highlights from these activities include the development of catalysts for the upgrading of lipids to hydrocarbons by means of decarboxylation/decarbonylation (deCOx), a study of bio-oil production from the fast pyrolysis of algae (*Scenedesmus*), and the application of pyrolytic gas chromatography coupled with mass spectrometry (Py-GC-MS) to the characterization of high lignin biomass feedstocks.

Table of Contents

Executive Summary

This project is aimed at the development of the biofuels industry in Kentucky by establishing a laboratory to develop improved processes for biomass utilization. Kentucky is well positioned to become a leading player in biofuels production: Kentucky's abundance of natural resources, including forestry wastes and agricultural residues, in addition to crops such as corn and soybeans, offers a huge resource of available biomass. The facility is based at the University of Kentucky Center for Applied Energy Research (UK CAER) and Department of Biosystems and Agricultural Engineering (BAE). The laboratory has been conceived as an open access facility, such that its equipment is available to researchers in other Kentucky institutions working in the field of biofuels. The development of a biofuels facility represents a significant expansion of research infrastructure, and will provide a lasting resource for biobased research endeavors at the University of Kentucky.

In order to continue to build research capacity, several major items of equipment were acquired for the Laboratory, including an anaerobic digester (for conversion of algae biomass to methane); a high pressure/high temperature pressure reactor for thermochemical conversion experiments employing lipids; HPLC and GC/MS instruments required for studies pertaining to lignin utilization for the production of fuels and chemicals, as well as the upgrading of lipids; a pyrorobe pyrolyzer unit (for biomass pyrolysis studies); and a IR spectrometer equipped with an environmental DRIFTS cell (for in situ catalyst studies). Initial research at the laboratory has focused on three technical areas: (i) the identification of algae strains suitable for oil production, utilizing flue gas from coal-fired power plants as a source of CO_2; (ii) the conversion of algae to biofuels; and (iii) the development of methods for the analysis of lignin and its deconstruction products.

To facilitate research aimed at the identification of algae strains suitable for oil production, four different culture systems were assembled. These permit the cultivation of algae in a controlled environment, utilizing synthetic flue gas. A particular objective was to identify the optimal culturing conditions for *Scenedesmus* sp., which in separate work is being used in a University of Kentucky project aimed at recycling CO_2 emissions. Studies were conducted to identify the optimal pH, growth media and water source for *Scenedesmus* sp., while a screening study was also successfully performed in order to identify promising strains for use under winter conditions (*Scenedesmus* being most suited to warm weather conditions).

Research on the conversion of algae to biofuels included the production of bio-oil from the fast pyrolysis of a dried microalgae feedstock. Product analysis showed the various fractions of bio-oil produced were, in certain respects, comparable to pyrolysis products from wood and other microalgae species. Indeed, the oxygen and moisture contents of the products were typical of pyrolysis oil produced from lignocellulosic feedstock. However, the average total acid number of the oil was lower than for bio-oil produced from wood pyrolysis. Furthermore, the products possessed a relatively high nitrogen content due to the high protein content in the algae feedstock. Anaerobic digestion was also examined as a means of valorizing algae, specifically, for the production of biogas. Experiments were performed at a scale of 0.5 – 4 L and included evaluation of biomethane gas potential (BMP) with and without algae pre-treatment (to lyse the algae cells).

The extraction and upgrading of algal lipids to liquid fuels represents another option for the utilization of algae. Work performed in our laboratory has shown that good yields of fuel-like hydrocarbons can be obtained from the fatty acids and the triglycerides that constitute algae

and vegetable oils *via* $deCO_x$. This approach show several advantages over hydrotreating, which is the method currently employed to achieve this transformation. Indeed, whereas hydrotreating necessitates high pressures of hydrogen and problematic sulfided catalysts, $deCO_x$ can proceed under considerably low hydrogen pressures and over simple metal catalysts. Although initial reports on this alternative deoxygenation approach focused on the use of catalysts comprising costly Pd or Pt, our work has shown that inexpensive Ni-based catalysts can offer $deCO_x$ performance comparable to formulations based on these precious metals. Advances have also been made with regards to the materials used as catalyst supports, as reports by other workers had focused on the use of activated carbon as the carrier in $deCO_x$ catalysts. Given that these catalysts are susceptible to deactivation by the accumulation of carbonaceous deposits on their surface and the use of a carbon support both complicates the study of spent catalysts *via* thermogravimetric analysis (TGA) and precludes the regeneration of the catalyst through the combustion of these deposits, efforts were made to develop non-precious metal catalysts comprising oxidic supports. Notably, our work has shown that Ni supported on oxide carriers and hydrotalcite materials has the ability to rival – and in some cases outperform – carbon-supported Pd, Pt, or Ni. The analysis of the spent catalysts comprising Ni on oxidic supports has allowed us to show that catalytic performance is determined by the interplay between hydrogen partial pressure and catalyst acidity, an effect which has been observed to be feed-dependent and explainable in terms of catalyst fouling. Finally, recycling studies have shown that the entirety of the activity and selectivity of Ni-based catalysts can be regained by treatment in hot air – the catalyst regeneration approach favored by industry due to its low cost and simplicity.

The deconstruction of lignin represented the third focus area. In order to identify and examine feedstocks that possess naturally high lignin content, pyrolytic gas chromatography coupled with mass spectrometry (Py-GC-MS) was employed. The resulting pyrograms showed that walnut shells, coconut shells, olive pits and switchgrass vary in their lignin and hollocellulose content, causing a variation in pyrolysis product distribution. Switchgrass contained the least amount of lignin and coconut shells the greatest; the latter also showed a much larger increase in the production of phenol when compared to pyrolysis of the biomass types. Our studies have also shown that Py-GC-MS can be used to obtain reliable values of the ratio of sinaply:guaiacyl (S:G) monomeric units present in lignin. The S:G ratio is an important value in the pulping industry because of its influence on sugar recovery from biomass. The relative abundance of these two monomers may also influence the products formed during pyrolysis of biomass which can influence the potential production of fuel and other chemicals from pyrolysis oil.

1. **General Introduction**

The principle objective of this project was the establishment of a laboratory dedicated to the development of improved processes for biomass utilization, with the goal of supporting the development of the biofuels industry in Kentucky. Kentucky is well positioned to become a leading player in biofuels production: Kentucky's abundance of natural resources, including forestry wastes and agricultural residues, in addition to crops such as corn and soybeans, offers a huge resource of available biomass. This new facility is based at the University of Kentucky Center for Applied Energy Research (UK CAER) and Department of Biosystems and Agricultural Engineering (BAE), and constitutes an "open" laboratory, i.e., its equipment is available to other Kentucky researchers working in the area. The development of a biofuels facility represents a significant expansion of research infrastructure, and will provide a lasting resource for biobased research endeavors at the University of Kentucky. Emphasis is placed on working with local biofuel producers in order that research findings can be readily implemented at the industrial scale.

Bearing in mind Kentucky's agricultural and forestry resources, and taking into account the fact that Kentucky possesses a disproportionately large CO_2 footprint due to its many (mainly coal-fired) power stations, this project focused on building research capability at the laboratory in the following technical areas:

- The identification of algae strains suitable for oil production, utilizing flue gas from coal-fired power plants as a source of CO_2;
- The conversion of algae to biofuels;
- Method development for the analysis of lignin (derived from forest and agricultural residues, as well as bioenergy crops) and its thermochemical deconstruction products.

Towards these goals, the necessary laboratory instrumentation was acquired and installed. As detailed below, these tasks were duly completed, after which activities focused on the application of these facilities to the foregoing research areas.

2. Results and Discussion

2.1. Laboratory set-up and utilization

The following major equipment items for acquired for the UK Biofuels Laboratory:

Agilent 7890A Gas Chromatograph: This instrument was purchased to fulfill general gas chromatographic needs of the biofuels laboratory. These tests include fatty acid methyl ester identification (ASTM D6584) as well as other methods developed in-house for glycerol carbonate quantification, etc. In addition, the instrument was retrofitted to enable Simulated Distillation analysis for boiling point distribution determination (ASTM D2887); this required the acquisition of an Agilent Multimode inlet which can be used for cryogenic GC work. State-of-the-art Simulated Distillation software from Separation Systems, Inc. was purchased to properly interpret the data.

Agilent 7890A GC – 5975C MSD with CDS 5200 Pyroprobe: This instrument was originally intended for liquid samples, such as algae pyrolysis oils; however, it was retrofitted to interface with a CDS 5200 pyroprobe. This allowed for the pyrolysis deconstruction products of a variety of high-lignin biomass sources, such as walnut shells and switchgrass, to be analyzed in line with the reaction.

Agilent 3000A Micro-GC (Refinery Gas Analyzer): Two instruments were acquired; each instrument has four GC columns (molecular sieve, Alumina, PoraPLOT U and OV-1) that run in parallel to analyze low molecular weight species (H_2, N_2, O_2, CO, CO_2, hydrocarbons, etc.).

Agilent 1260 Infinity HPLC: This instrument is almost exclusively used for gel permeation chromatography, but can potentially be used for lipid analysis or a number of other applications. It is equipped with a UV-Vis diode array detector, a Corona charged aerosol detector, an i-chem explorer heated and stirred sample tray, a fraction collector and a quad pump which allows for the use of four solvents.

ThermoScientific Nicolet 700 FT-IR Spectrometer: Beyond the general functionality of an IR spectrometer, this equipment has 2 accessory packages that enhance its capabilities: 1. ATR assembly and 2. DRIFTS accessory incorporating a temperature controlled reaction chamber. The latter allows for in-situ analysis of gas-solid phase reactions which aids in catalyst characterization.

Dionex Ion Chromatography System: This instrument is used to determine the nutrient uptake of algae. Analysis of nutrient water containing cations (e.g., Ca^{2+}, K^{+} and Mg^{2+}) as well as anions such as NO_3^- can aid in the development of optimal nutrient systems.

TA Discovery Series Thermogravimetric Analyzer: This TGA has an autosampler allowing for high throughput sequences. Applications for this instrument include catalyst characterization, thermolysis, pyrolysis and combustion.

Metrohm 809 Titrando titroprocessor and Anton Parr DMA 4100 digital density meter: These instruments were acquired for the determination of the total acid number (TAN) of biofuels and for the determination of biofuel density, respectively.

Ankom Gas Production System Anaerobic Digestor: This anaerobic digestor was purchased to facilitate studies pertaining to the conversion of algal biomass to methane.

Dionex ASE 350 Accelerated Solvent Extractor: This unit uses 100ml extraction cells and is used for lipid extraction from algae.

Other: General purpose laboratory equipment was purchased to support the day to day operations of the lab. Examples include an explosion proof refrigerator and freezer, two rotary evaporators, an HPLC pump, a vacuum oven, pH meters, stirred heating mantles, a muffle furnace, mass flow controllers, valves, tubing, etc.

Fixed bed reactor: This reactor was constructed on-site and is used to test solid base catalysts for biodiesel production. The reactor is rated to 250°C and 1450 psi.

Fixed bed reactor: This reactor was purchased from Parr instrument Company for studies pertaining to the catalytic upgrading of vegetable oils, algae oil and model triglycerides to hydrocarbon fuels.

Mechanically stirred reaction vessels: A variety of autoclaves were acquired which are used on a daily basis for thermochemical upgrading studies using biomass (oils, fats, lignin) or model compounds as the feed.

Extruder: Renovation was completed on an existing Killian 2" single screw extruder to facilitate biomass liquefaction studies. The existing metering screw was exchanged for a new stainless steel uniform flight screw in an attempt to minimize coking and avoid dead zones in the reactor.

Algal Growth System: Four culture systems were set up and made operational, comprising: (i) 21 x 500 ml flasks on a shaking table (for tests with SOx and simulated flu gas); (ii) 500ml flasks with temperature platform (for testing temperature dependence between algae strains); (iii) 500ml flasks (27 per rack x 4 racks) in a controlled environment chamber (for tests focusing on media optimization, PBR construction materials and waste-water treatment); and (iv) pilot scale reactors (6 x 10 L reactors for scale-up studies).

In keeping with the open laboratory objective, experiments and sample analysis were performed in the Laboratory at the request of other institutions, as well as other research groups within the University of Kentucky. These requests included the following:

- Süd-Chemie (now Clariant; Louisville, KY): Simulated Distillation Gas Chromatography analysis of lube oil samples on multiple occasions.

- Audubon Sugar Institute (Louisiana State University): Biological and agricultural engineering requested digital density measurements on ca. 30 samples of biofuels produced from sugarcane.

- American Science & Technology, Inc. (Wausau, WI): GC analysis of biodiesel samples, bomb calorimetry of biomass samples.

- Eclipse Renewables (Houston, TX): Evaluation and steam activation of carbon derived from fast pyrolysis.

- Sapphire Energy (San Diego, CA): Thermochemical processing of algae.

- University of Kentucky Department of Biosystems and Agricultural Engineering: micro-GC analysis of gas sampled from biomass storage silos.

- University of Kentucky Department of Chemistry: Several analyses were performed including Py-GC-MS of lignin model compounds that had undergone oxidation reactions and HPLC on silyl polymers to determine the molecular weight distribution.

- University of Kentucky Department of Plant and Soil Sciences: Autoclave equipment was used in order to hydrogenate partially cyclopropanated soy oil. A catalyst was also provided, together with advice on appropriate reaction conditions.

- Kentucky Geological Survey (KGS): GC-MS and Simulated Distillation GC analysis of coal tar.

- University of Kentucky Center for Applied Energy Research (UK CAER): members of the Power Generation and Utility Fuels Group submitted samples for gas chromatographic analysis (consisting of gas and liquid bio-oil samples produced from the fast pyrolysis of biomass).

To further publicize the fact that the UK Biofuels Laboratory is available to external institutions, the CAER public relations department created a website, http://www.caer.uky.edu/renewablefuels/lab.shtml, outlining the laboratory's analytical capabilities and providing appropriate contact details.

2.2. Development of methods for the analysis of lignin and its deconstruction products

2.2.1. Pyrolysis-GC-MS

Introduction

This task focused on the deconstruction of lignin, to guide the development of improved processes for the efficient processing of lignin into fuels, as well as valuable chemicals. While cellulose has received much attention for deconstruction via biochemical [1,2] and thermochemical means [3,4], lignin, as the second most abundantly renewed biopolymer on the planet, is often looked upon as a waste product due to its complex structure and recalcitrance. However, lignin contains structural units that could serve as a source of fuels and high-value chemicals [5], if means can be found to free those structural units from the polymer.

In order to identify and examine feedstocks that possess naturally high lignin content, we have employed pyrolytic gas chromatography coupled with mass spectrometry (Py-GC-MS). The use Py-GC-MS can provide valuable insight into the structure and composition of lignin through the analysis of the products obtained when the latter is pyrolyzed. Parenthetically, this analysis can also provide valuable information regarding the potential of a particular lignin sample as a fuel source. Given that Py-GC-MS allows for lignin to be pyrolyzed in the presence of a catalyst, this technique can also be used to screen potential catalysts for the pyrolytic depolymerization of lignin. With this in mind, a Pyroprobe 5200 pyrolyzer with thermal desorption and reactant gas operation capabilities was purchased from CDS Analytical, Inc. and interfaced with an existing GC-MS. Subsequently, the GC-MS was calibrated using appropriate standards to allow quantification of the yields of the main products expected (phenol, m-cresol, p-cresol, guaiacol, syringol, etc.) and used to identify the differences in lignin composition in biomass such as switchgrass, walnut shells, coconut shells, peach pits and olive pits [6]. In addition to analyzing the whole biomass, lignin has also been extracted from the biomass sources and analyzed separately using Py-GC-MS. In order to understand and calibrate for the differences in pyrolysate distributions between different lignin monomers, sinapyl and coniferyl alcohol were also pyrolyzed alone and in mixtures [7]. The composition and the relative amounts of the pyrolysis products are used to distinguish different lignin types and to determine whether a given biomass source is capable of producing specific pyrolysis products. These findings have been published [6,7] and further optimized in an effort to obtain accurate and precise analysis of lignin and biomass pyrolysates.

Materials and Methods

Biomass and sample preparation: Biomass was ground, degummed and analyzed prior to lignin extraction. Lignin was extracted by mixing 1 g biomass with 20mL of 85% formic acid with 0.2% HCl at 65^{o}C for 24 h. The residual pulp was filtered, washed with formic acid and the liquid filtrate was rotary evaporated to recover formic acid. Then, water was added to the material remaining after evaporation to dissolve hydrolyzed hemicellulose, leaving behind lignin as a precipitate. The lignin was filtered, washed with water and dried overnight in an over at 80^{o}C.
1 mg of the ground (45-150 μm) biomass, and lignin and other reference samples (i.e. cellulose, xylan, sinapyl alcohol, coniferyl alcohol and sinapyl/coniferyl mixtures) were analyzed in quartz cells packed with quartz wool. The samples were heated to 100°C for 10 s in the probe prior to analysis in order to remove any residual water.

Pyrolysis: Experiments were performed using a Pyroprobe Model 5200 (CDS Analytical, Inc.) connected to an Agilent 7890 GC with an Agilent 5975C MS detector. The pyroprobe was run in trap mode under He atmosphere. Pyrolysis was conducted at 650°C (1000°C/s heating rate) for 20 s. The valve oven and transfer lines were maintained at 325°C. The column used in the GC was a DB1701 (60m x 0.25mm x 0.1 µm) and the temperature program was as follows: 45°C for 3 min., ramp to 280°C at 4°C/min and hold for 10 min. The flow rate was set to 1 mL/min using He as the carrier gas. The inlet and auxiliary lines were both maintained at 300°C and the MS source was set at 70 eV. The GC-MS was calibrated for a number of phenolic compounds including phenol, 2-methoxyphenol, 2-methoxy-4-methylphenol, 2,6-dimethoxyphenol, vanillin, syringaldehyde and 2-methoxy-4-vinylphenol. Pyrolysis products were analyzed according to retention times and mass spectra data obtained from a NIST library.

Results and Discussion

Whole biomass pyrolysis yielded products associated with hemicellulosic, cellulosic and lignin fractions within the biomass. Holocellulosic pyrolysis products included furan derivatives, furfural, acetic acid and other short chain oxygenated compounds. These compounds typically elute earlier in the pyrograms than the lignin-based pyrolysates. Lignin pyrolysis products included methoxyphenols and other aromatic compounds derived from the monomeric units coumaryl, coniferyl, and sinapyl alcohol within the lignin structure. Table 1 shows selected marker compounds for both lignin and holocellulosic fractions with their retention times and sources as they appear in the pyrograms. The origin of the pyrolysates was validated by pyrolyzing cellulose, xylan, lignin extracts and lignin monomers, and by comparison with the results of other published studies [8,9].

Coconut shell pyrolysis produces much higher amounts of phenol and less 2-methoxyphenol than the other samples as indicated by both whole biomass pyrolysis and pyrolysis of lignin extracted from the samples. Pyrolysis of coconut shell lignin is shown in Figure 1 and shows that pyrolysis of the lignin fraction also creates a small amount of acetic acid and furfural. This could be due to leftover hemicellulose in the lignin fraction. It also shows a large amount of phenol production, whereas the amount of 2-methoxy-4-methylphenol is less than that produced from olive pits or walnut shells. This result indicates that the lignin extracted from coconut shell shows similar composition and structure to the original biomass, although some differences are noted. These changes are likely the result of changes made in the lignin structure during the extraction process. Coconut shell lignin pyrolysis also produced more 2,6-dimethoxyphenol than the other lignin samples. Given that 2,6-dimethoxyphenol is considered to be a marker for sinapyl alcohol, the result suggests that coconut shells may contain higher amounts of the sinapyl alcohol monomer in the lignin structure [10].

Figure 2 shows a pyrogram of walnut shell pyrolysis at 650°C. Isoeugenol and 2-methoxy-4-vinylphenol are the primary products resulting from the lignin pyrolysis within the biomass where acetic acid and furfural are produced primarily from the hollocellulosic fraction. Walnut shells, peach pits and their respective extracted lignin pyrolysis show that these biomass samples contain much fewer sinapyl-based lignin monomers within the lignin framework than coconut shells or olive pits because they produce fewer sinapyl-based pyrolysates. Olive pits and the extracted lignin pyrolysis (pyrograms not shown) produced about the same area percent contribution of sinapyl and coniferyl-based compounds. Again, the distribution of pyrolysates from the lignin fraction of the whole olive pit biomass varies slightly from the lignin extract. These results indicate that changes were made to the lignin structure during the extraction process or the extraction process only yielded only a fraction of the lignin and that it was not

representative of the whole. Further analysis of the remaining pulp products is under investigation in order to provide more information on the source of these differences.

Table 1. Select compounds identified in pyrograms obtained from biomass and lignin pyrolysis.

Compound	Retention time (min)	Source
acetic acid	8.5	Holocellulose
1-hydroxy-2-propanone	9.8	Holocellulose
furfural	15.5	Holocellulose
2 (5H) furanone	21.7	Holocellulose
4-hydroxy-5,6-dihydro-2H-pyran-2-one	22.8	Holocellulose
phenol	24.5	Lignin
2-methoxyphenol	25.3	Lignin
2-methylphenol	26.4	Lignin
2-methoxy-4-methylphenol	29.0	Lignin
4-ethyl-2-methoxyphenol	32.2	Lignin
2-methoxy-4-vinylphenol	33.7	Lignin
2,6-dimethoxyphenol	35.4	Lignin
2-methoxy-4-(1-propenyl) phenol (T)	37.9	Lignin
2,6-dimethoxy-4-methylphenol	38.3	Lignin
vanillin	38.6	Lignin
2,6-dimethoxy-4-vinylphenol	42.1	Lignin
2,6-dimethoxy-4-(1-propenyl)phenol (E)	45.6	Lignin
4-hydroxy-3,5-dimethoxybenzaldehyde	47.0	Lignin

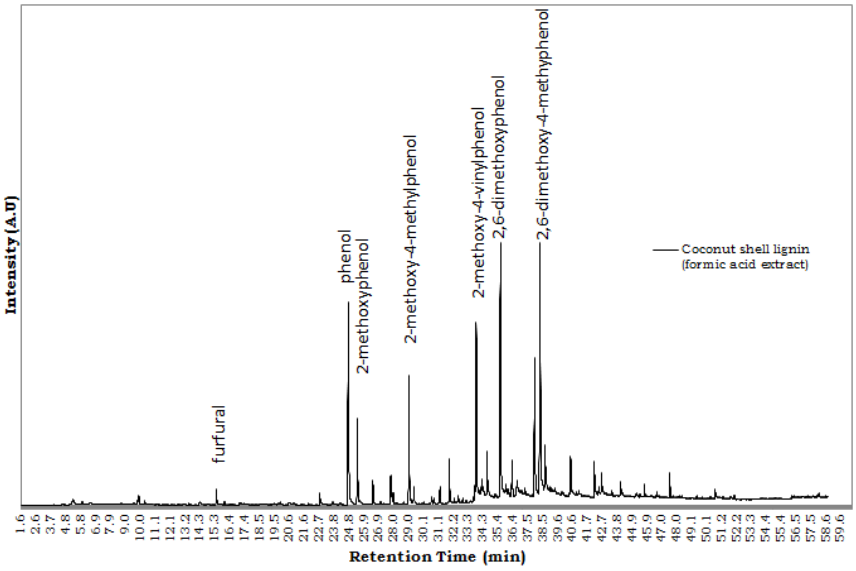

Figure 1. Coconut shell lignin pyrogram.

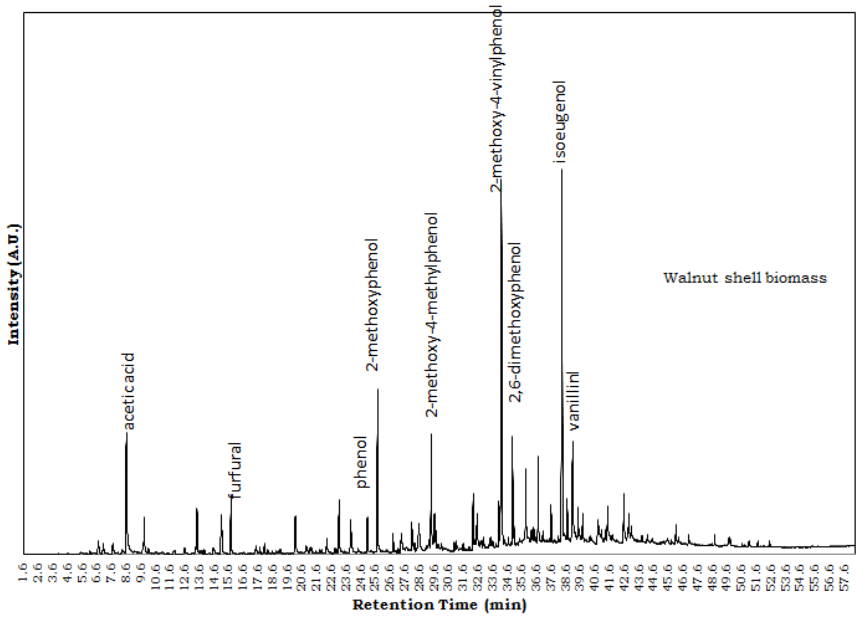

Figure 2. Walnut shell pyrogram.

Pyrolysis-GC/MS of sinapyl and coniferyl alcohol, as well as mixtures of the two was also performed in order to elucidate the origin of certain lignin-based pyrolysates. The most abundant compounds produced from coniferyl alcohol are 3-(4-hydroxy-3-methoxyphenyl)-2-propenal, trans-isoeugenol, vanillin, 2-methoxy-4-propylphenol, and homovanillic acid. The most abundant compounds produced from sinapyl alcohol include 2,6-dimethoxy-4-vinylphenol, 4-hydroxy-3,5-dimethoxybenzaldehyde, 2,6-dimethoxy-4-(1-propenyl)phenol, 4-propylsyringol and 4-methylsyringol. Pyrolysis of the mixtures of the two alcohols produced practically no new compounds, indicating that the two starting materials did not react with each other [7].

The total ion chromatogram area % of certain marker pyrolysates for each alcohol were summed and used to calculate sinapyl:guaiacyl (S:G) ratios in the mixtures; these ratios were then plotted against the actual molar S:G ratios of the starting material. 13 coniferyl alcohol marker pyrolysates and 9 sinapyl alcohol marker pyrolysates provided acceptable linear correlation, as shown in Figure 3, whereas several other marker groups chosen did not correlate to the actual S:G ratio in the starting material. Having obtained the pyrolysis profile of the various S:G mixtures, marker pyrolysates for the calculation of the S:G ratio in lignin can be carefully selected according to unique samples. These marker groups can then be calibrated against known S:G ratios to provide analysis of the actual S:G ratio of lignin in biomass [7].

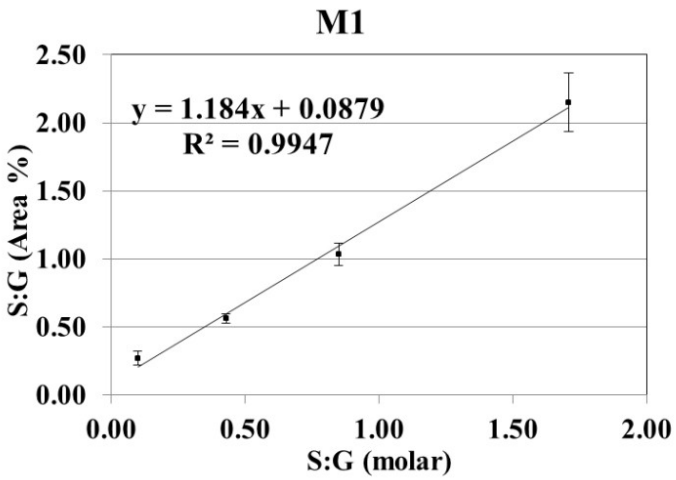

Figure 3. Sum area percent S:G ratio vs. molar S:G for the marker compound group consisting of the 13 most abundant coniferyl-based pyrolysates and 9 sinapyl-based pyrolysates.

Conclusions

In conclusion, pyrograms show that walnut shells, coconut shells, olive pits and peach pits vary in their lignin and hollocellulose content and structure, causing a variation in pyrolysis product distribution. Pyrolysates from whole biomass contained large amounts of acetic acid and furfural whereas these compounds are produced only in small amounts from the corresponding lignin fractions. Overall, these results serve to illustrate the potential of high-lignin endocarp feedstocks such as coconut and walnut shells, which are readily available as agricultural waste from horticultural crops, to generate valuable chemicals by thermochemical deconstruction.

2.2.2. Gel permeation chromatography (GPC)

As indicated above, an Agilent 1260 HPLC was procured for the analysis of lignin and lignin oxidation products. This HPLC system came with online diode array detection (DAD), as well as an ESA Charged Aerosol Detector (CAD) for analytes that may not have a chromophore. The system was initially configured to perform size exclusion chromatography using an aqueous reverse phase mobile phase on a Polymer Standard Services (PSS) Suprema Linear S column. The column was then calibrated using polyethylene glycol (PEG) as a MW standard. Literature reports had claimed the use of a 0.1 M mobile phase of sodium hydroxide [11]. However, this was not feasible with our system due to the CAD detector being incompatible with alkali metals. We then decided to move towards the use of ammonium hydroxide in the mobile phase. This, however, gave only limited information about lignin structure due to its ability to completely dissolve lignin and to the very noisy baseline in the CAD detector which was suspected to be from the elevated pH.

After consulting with PSS about column/solvent compatibility we moved towards the use of a mobile phase composed of dimethyl sulfoxide/water. This, however, lead to a high back pressure and resulted in the need to slow our flow-rate and, in turn, increase our analysis run time. The decision was then made to change the mobile phase to a 50/50 mixture of DMSO/THF. This served two purposes. First, it relieved some of the back pressure on the

column and second it straddled lignin's reported Hildebrand solubility parameter range (20-29 $MPa^{1/2}$). DMSO and THF have Hildebrand Parameters of 24.5 $MPa^{1/2}$ and 18.6 $MPa^{1/2}$, respectively [12]. This allows for almost complete dissolution of organosolv lignin, thus providing a better representation of molecular weight shifts that may be occurring during lignin oxidation reactions (this having been a problem with other mobile phases).

Lignin analysis was found to be readily accomplished using the DAD detector at wavelengths of 280 nm and 320 nm [11]. The CAD detector has proved to be useful mainly in the determination of approximate molecular weight. This remains a somewhat challenging process as the determination of molecular weight is typically based on standards that are of the same or similar chemical composition and structure to the analyte. In the case of lignin this is an arduous process due to the lack of commercial molecular weight standards that accurately represent lignin's chemical structure. This, however, can be broken up into two parts: high molecular weight lignin and low molecular weight lignin. There are two distinct peaks in the HPLC spectra (Figure 4), one at early retention times circa 10 minutes (6 mL) and the other at late retention times (15 minutes, 9 mL) which correspond to high molecular weight and low molecular weight lignin, respectively. According to the molecular weight standards that are typically used (polystyrene sulfonate or polyethylene glycol), the late retention times would correlate to about 700 Da, or the size of a lignin trimer. In the case of low molecular weight lignin, polystyrene should be a fairly accurate measure of molecular weight given that the smaller lignin's structure more resembles polystyrene. However, this is not the case when it comes to high molecular weight lignin. We find this lignin to be at or above the elution volume of our column, meaning that anything in this region should be heavier than 100,000 Da. This is a phenomenon known as super-elution [11]. This is not a trivial measurement, given that it is based on size, not molecular weight. In this case we cannot measure the molecular weight of our lignin with any real sense of accuracy using commercially available molecular weight standards. To do so would require the use of the Mark-Houwink equation that relates all polymers, regardless of the molecular weight, to their hydrodynamic volume. To solve the equation, one would need the measurements from a light scattering detector and a viscometer, as well as a concentration detector (RI or UV/VIs).

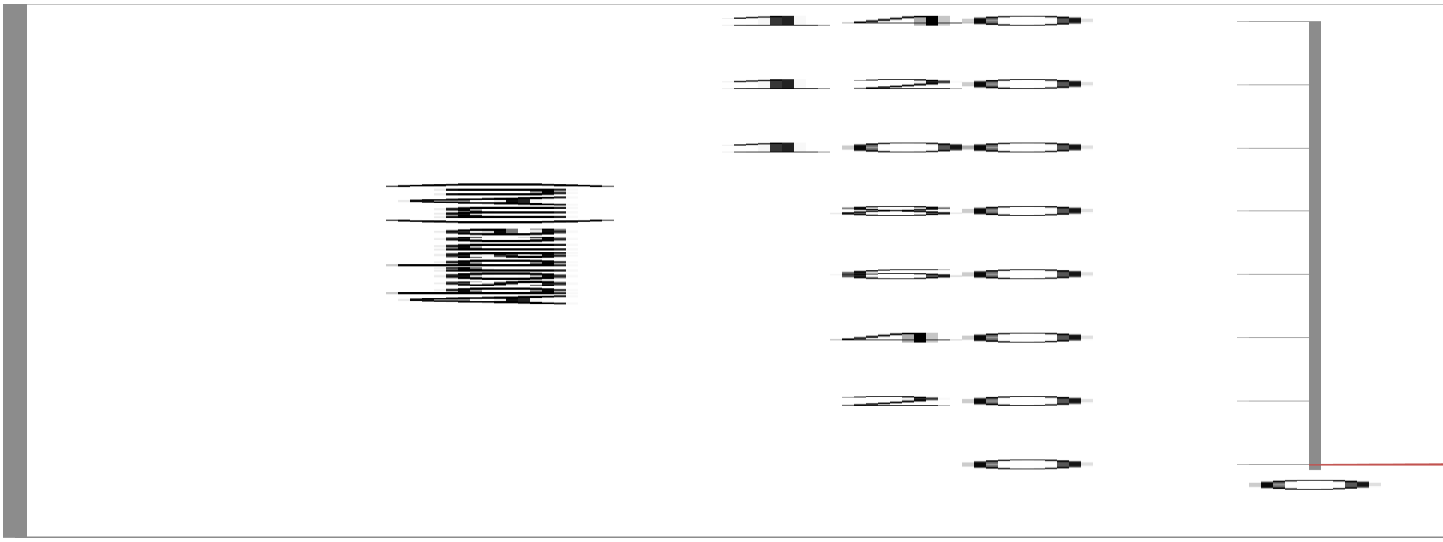

Figure 4. Size exclusion chromatogram of Organosolv lignin.

This leads to the question of why are there two peaks rather than just one. There are two potential explanations. Organosolv lignin occurs in two fractions, the first of which passes through the column without any hindrance whatsoever. This is deemed high molecular weight

lignin. One explanation for this observation is that the Organsolv lignin has the appearance of having a high molecular weight because it forms aggregates in solution that have a larger hydrodynamic volume that the individual molecules. In this case there are very few of column-solute interactions because the solute is not being retained at all. Secondly, Py-GCMS analysis indicates that the Organosolv lignin contains a fair amount of hemiceullose. Hemi-cellulose can have repeating units of 50-300 units. Given that a single unit has a molecular weight of 180 Da and that some (if not most) of the hemicellulose lignin should be covalently attached to the lignin, the high apparent molecular weight of this fraction is explained. Current work is aimed at differentiating between these two possibilities.

2.3. Development of algal strains for CO_2 capture from power plants

Four different algae culture systems were assembled for cultivation and associated experiments. The first consisted of multiple 500 mL flasks on a shaker table located in a walk-in hood. This setup was used for experiments such as the effect of SO_x and simulated flue gas on algae (Figure 5). The second system consisted of a temperature controlled platform housed in a sealed box. It can hold up to twelve 500 mL flasks for temperature dependent experiments employing multiple algae strains. The third setup was located in an environmental (temperature and humidity) controlled chamber with four shelving units; each held 27 flasks, that enabled four different experiments to be run simultaneously. Experiments included media optimization and growth studies for bioreactors comprised of different construction materials. The final system was a modified pilot-scale bioreactor (32 L) intended for larger scale and continuous experiments.

Figure 5. Algae culture system used in a simulated flue gas experiment with 21 flasks on a shaker table.

The first objective was to identify the optimal culturing conditions for the summer algae strain *Scenedesmus sp.*, which in separate work is being used in a University of Kentucky project aimed at recycling CO_2 emitted from coal-fired power plants. One of the first experiments conducted was media optimization. The standard growth media ("urea media") utilized commercial grade urea fertilizer as the nitrogen source. The final urea media composition

decided upon was 2 L of tap water, 0.275 g of urea, 0.0596 g of K_2HPO_4, 0.0542 g of Mg_2SO_4, and 0.01 g Na.EDTA.Fe.

Alternative nitrogen sources such as potassium nitrate (KNO_3) and ammonium nitrate (NH_4NO_3) were explored to enhance algae growth. At pH levels of 5, 6, 7 and 8, KNO_3 or NH_4NO_3 (at equivalent nitrogen concentration to the urea medium) was added separately to the standard media while keeping other macronutrients (P, K, Ca, Mg, etc.) the same. After 96 hours in triplicate flasks, *Scenedesmus* preferred urea as the nitrogen source and exhibited the highest growth rate at a pH value of 7 (Table 2).

Table 2. Growth rate of *Scenedesmus sp.* cultured in various media at pH 5, 6, 7, and 8

media/pH	pH 5	pH 6	pH 7	pH 8
urea	0.0155	0.0222	0.0244	0.0230
KNO3	0.0113	0.0131	0.0178	0.0162
NH4NO3	0.0114	0.0144	0.0159	0.0136

In addition, micronutrients such as boron, vanadium, and molybdenum could be beneficial in culturing *Scenedesmus*. In a comparison study with a control, they were added separately or together to the standard urea media. Results showed the addition of all three micronutrients improved growth rate. However, at this time, the increase in growth rate was not worth the added expense of the micronutrients.

Another effort to maximize growth rate was to identify the optimal pH level for *Scenedesmus*. In a buffered pH study, urea media was buffered to various pH values of 5 to 8 in increments of 0.5 in triplicate flasks for 96 hours. A follow-up study was also conducted using pH values of 7, 8, 9, and 10. The highest growth rate, and hence CO_2 uptake, was observed at a pH value of 7 - 8 (Figures 6 and 7).

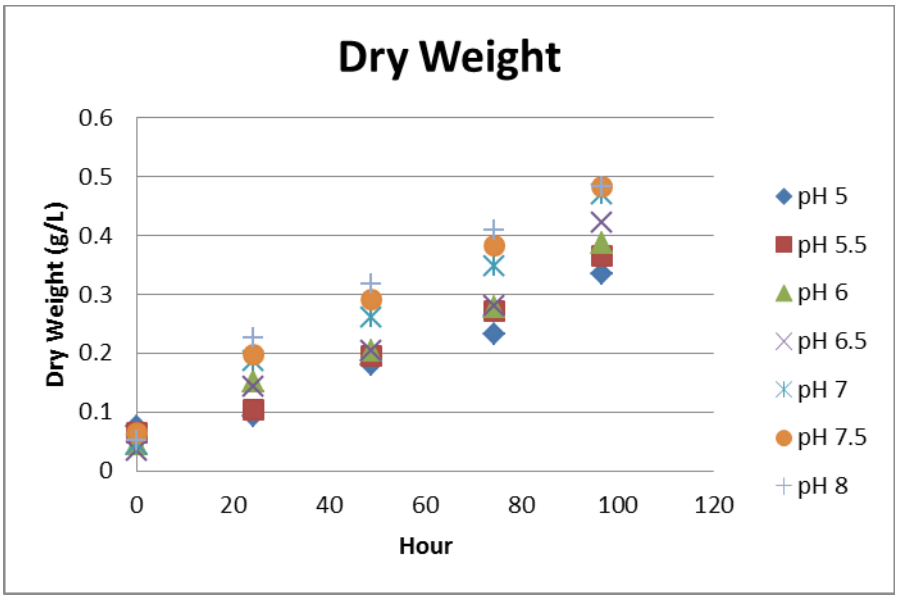

Figure 6. Dry weight of *Scenedesmus sp.* cultured in buffered urea media at pH 5-8 in increments of 0.5.

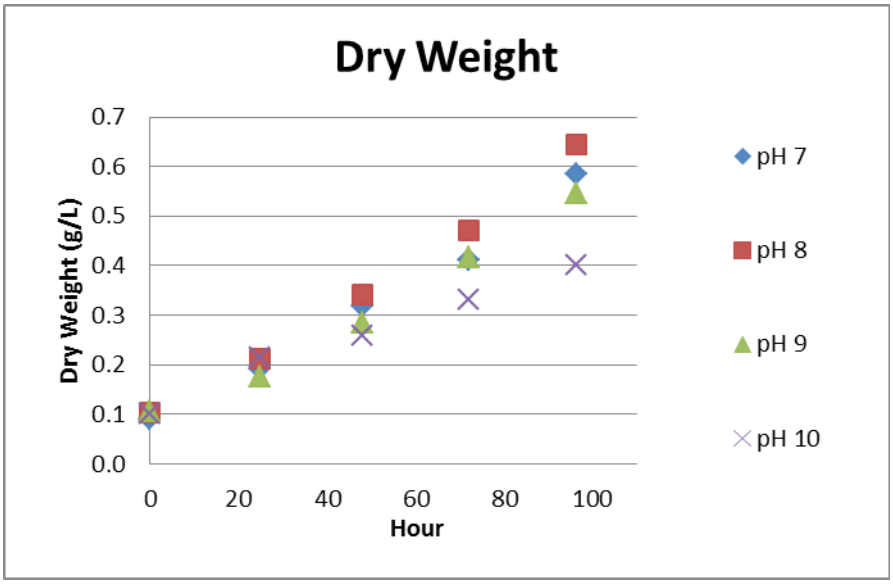

Figure 7. Dry weight of *Scenedemus sp.* cultured in buffered urea media at pH 7, 8, 9, and 10.

In a separate study, non-potable water was considered for *Scenedesmus* cultivation when city tap water was not available. Water was collected from an agricultural run-off pond near the University of Kentucky Center for Applied Energy Research. An initial comparison study between the pond water and city water in urea media showed the growth rate obtained from the pond water was less than the city water. Pond water was then submitted for elemental analysis to determine the chemical components in the water. Based on the report, water was supplemented with additional nitrogen, potassium, and micronutrients to match up with the standard media. Algae were cultured in both supplemented pond water and standard media for 96 hours. Once again, the growth rate obtained with the pond water lagged behind.

To continue the effort of utilizing pond water for culturing, another set of experiments was performed by doubling the amount of nitrogen and potassium added to the pond water. The resulting growth rate was noticeably higher than the previous result, although it was still less than the standard medium. Together, these results suggested that additional nutrients, other than the macronutrients nitrogen and potassium, were required for algae culturing and were responsible for the different results for city water and pond water.

In other work, three non-potable water sources available at the Duke Energy's East Bend power plant (located near Rabbit Hash, KY) were examined for *Scenedesmus* cultivation. Process water, well water (underground water flowing through aquifers), and condensate boiler water (similar to deionized water) were compared to city water in a growth study. The standard urea media was added to all four waters to ensure algae growth. Toward to the end of experiment, well water displayed the highest growth rate followed by the city water, process water, and condensate boiler water. Well water was the best choice for East Bend algae cultivation (Figure 8) and is currently being used in a demonstration scale photobioreactor at the East Bend station.

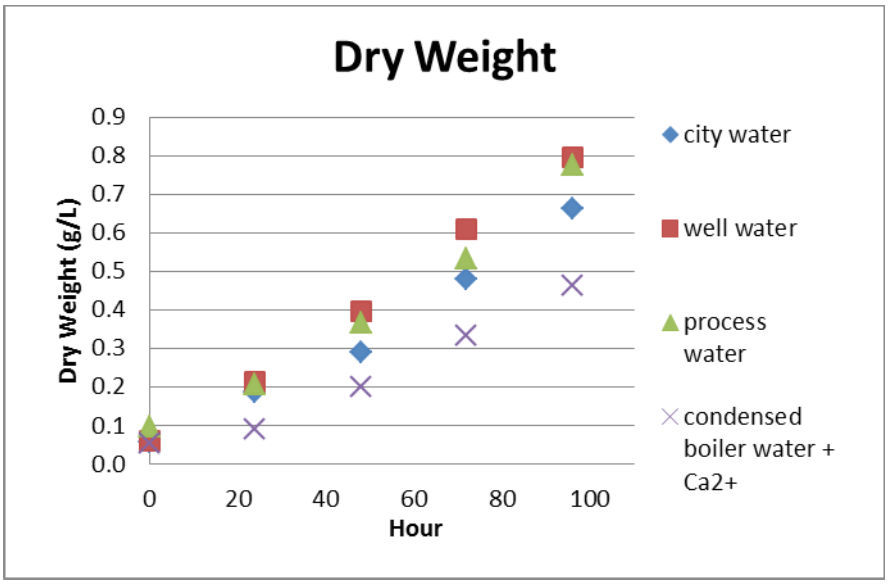

Figure 8. *Scenedesmus sp.* cultured in non-potable water sources available at Duke Energy's East Bend power plant.

Finally, a screening for an algae strain suited to culturing in winter conditions was completed. Sixty strains were obtained from the UTEX Collection of Algae from the University of Texas in Austin, Texas. They were cultured in two different media (Bold's basal media and modified urea media) and pH values (5.5 and 7.5) in small culture volume (100 mL). All strains were cultured at 16-18°C and illuminated in a 12:12 hour light:dark cycle for 30 days (until a plateau was reached). Growth measurement was based on absorbance reading measured at 450 nm wavelength. At the end, ten strains (*Haematococcus droebakensis, Bracteacoccus minor, Neochloris wimmeri, Chlorella luteoviridis, Chlorella sorokiniana, Chlorella regularis, Chlorella kessleri, Stichococcus bacillaris, Chlorella vulgaris,* and *Tetraspora sp.*) were identified based on their promising results.

2.4. Utilization of algae

2.4.1. Anaerobic digestion

Dried *Scenedesmus sp.* (15.6% total solid, 90.6% volatile solid of the total solid*)* was used as substrate in anaerobic digestion for methane production. As shown in Figure 9, multiple sealed 500 mL bottles containing dried algae and active microorganisms (sludge) were incubated at 38°C water bath. The resulting biogas was captured and passed through tubing to sodium hydroxide filled bottles for CO_2 removal and into calibrated flow cells for continuous online qualification of biogas. The methane content was analyzed with a Perkin Elmer Clarus 600 Gas Chromatograph on a PLOT Q column and a thermal conductivity detector.

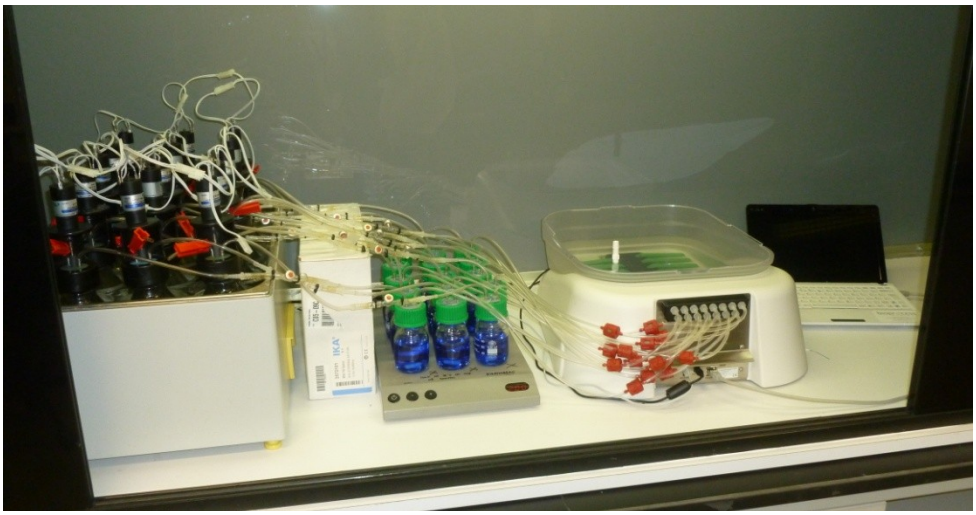

Figure 9. Anaerobic digestion system.

A preliminary experiment was conducted by filling three algae bottles (6 g volatile solid/L) and three control bottles (no substrate) with active sludge and incubating them at 38°C for 42 days. Methane production of 228 mL and 215 mL accumulated methane/g of volatile solid (VS) was collected in the first two sets of data. The last set of data collection was terminated prematurely due to a gas leak (Figure 10). A second set of experiments was performed using the same batch of dried *Scenedesmus* with the aim of completing and replicating the previous test. By the end of 42 days, an average of 220 mL accumulated methane/g VS was obtained, similar to the result in the previous study.

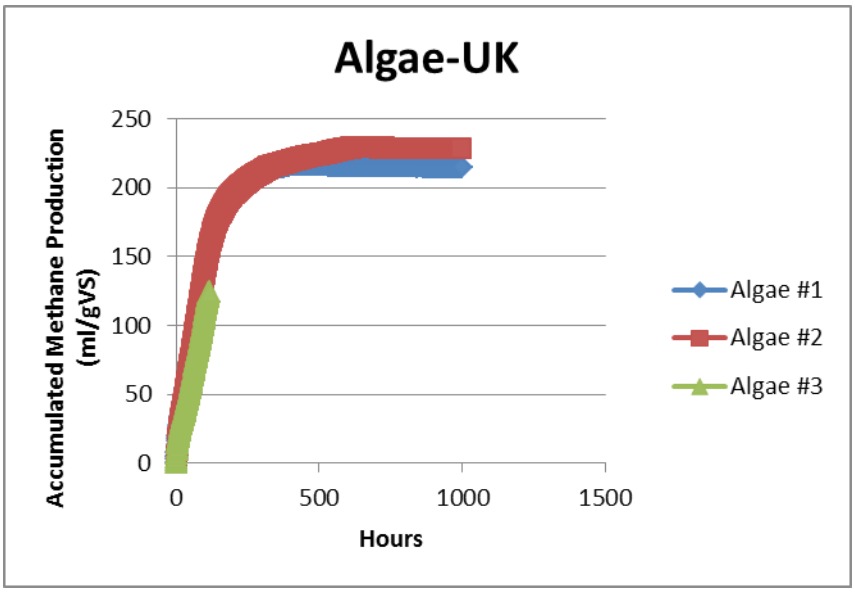

Figure 10. Methane production obtained from anaerobic digestion of dried *Scenedesmus sp.*

Scaling up from the 500 mL bottles, a new 4 L digester equipped with continuous stirring was assembled at Kettering University in Flint, Michigan (under subcontract). The digester was initially seeded with digestate obtained from another digester and fed with active sludge until the reactor was stabilized and ready for use. On a daily basis, dried algae mixed with spent growth

media (obtained from the supernatant of centrifuged fresh algae) was added to the reactor. Biogas produced was continuously collected and measured. Both digestate and biogas was quantified weekly.

Initial test results indicated the reactor was acclimated to the algae, resulting in an increase in specific gas production and methane percentage and contained a low level of volatile fatty acids (VFAs) and 60% degradation rate. The hydraulic retention time (HRT) was maintained at 30 to avoid ammonia inhibition and the nitrogen levels were below inhibitory range. The phosphate levels were also measured to determine the feasibility of integrating the digestate as algal media. However, the pH and alkalinity dropped.

On a regular basis, centrifuged algae mixed with supernatant were added to the reactor to support a continuous digestion. Toward the end of second month of running, the ammonia level and VFAs began to build up inside the reactor. In an effort to lower the ammonia level, pH was dropped below 7.4 with hydrochloric acid until the levels of ammonia and VFAs were lowered and stabilized. The specific gas and methane production was stabilized as well. However, the pH and alkalinity continued to fluctuate.

After the third HRT, the digester was switched over to using algae as the substrate with the organic loading rate (OLR) held constant or increased. Only one HRT was completed before foaming occurred due to the accumulation of ammonia. Foaming stopped once the OLR was lowered with the addition of decanted algae to the reactor. Specific gas and methane production was continuously measured.

The load rate versus gas production for the fresh algae showed that with increasing OLR the biogas production increased, although it represented the same amount of biogas per volatile solids (Figure 11).

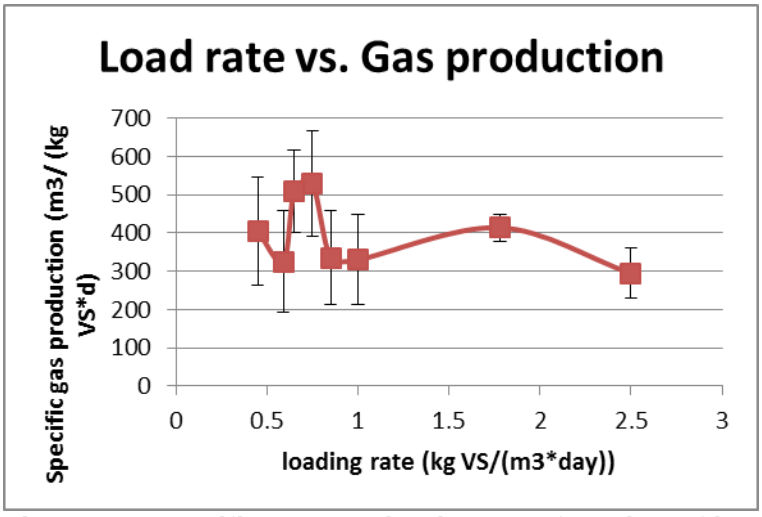

Figure 11. Specific gas production as a function of loading rate for fresh algae.

Due to the rigid cell wall of *Scenedesmus sp.* (composed of cellulose and other polysaccharides), digestion of polysaccharides into sugars - ultimately generating methane biogas - was limited. Pretreatment of algae was performed to hydrolyze the polysaccharides to bring them into a form more readily available for digestion. *Scenedesmus,* in the form of fresh, flocculated, and flocculated and dried algae, was pretreated with a combination of sodium hydroxide (NaOH) and elevated temperatures. The highest increase in digestibility was 17%,

achieved by incubating algae in 12% NaOH solution at 90°C for 60 min. However, the biomethane production (BMP) for the pretreated algae was not significantly different from the untreated algae (Figure 12).

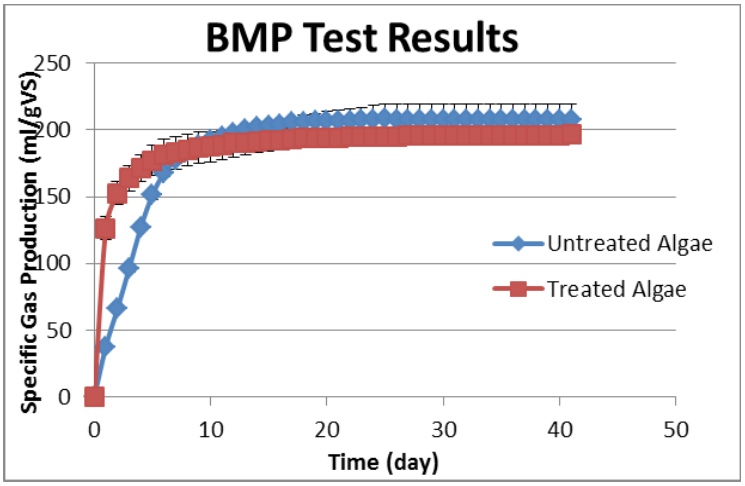

Figure 12. Specific gas production as a function of time for treated and untreated algae.

At this point, the reactor has acclimated to digesting algae. We have weaned the reactor off the acid and the ammonia levels are stabilizing. We have completed 3 HRT to completely change over the reactor contents to algae. We completed one HRT with the OLR held constant or increased. We have completed three HRTs with the OLR fluctuating based upon the feed. The last HRT was done with pretreated algae.

The reactor experienced foaming problems when the OLR was held constant. That may have been due to ammonia accumulation. Once the OLR was dropped when the decanted algae was fed, the foaming stopped. There is no significant difference in gas production among the tested OLRs. The VS destruction rates for raw and pretreated algae were 41.8% and 83.6%, respectively. It seems more algae are decomposed after the mild pretreatment. In addition, fluorescent pictures were taken to quantify the effect of pretreatment on algae cell walls. The number of dead cells with disrupted cell walls was, in fact, increased with pretreatment severity, but it did not correlate with the digestibility of the algae (Figure 13).

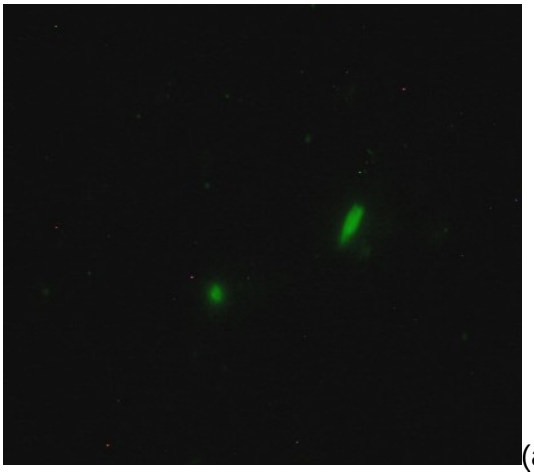
(a)
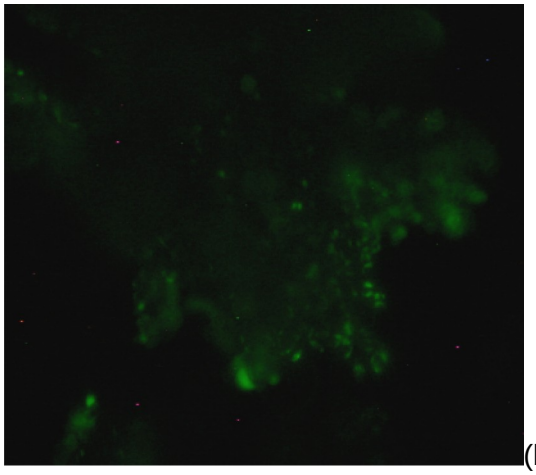
(b)

Figure 13. Fluorescent pictures of algae, where the green indicates cell wall degradation. Without (a) and with (b) pretreatment are both shown.

2.4.2. Fast pyrolysis of algae

Introduction

Fast pyrolysis of microalgae was investigated as a potential method for conversion of algae into liquid products capable of being further processed into valuable fuels. In order ascertain the viability of producing liquid fuels from whole algae (i.e., avoiding the necessity of extracting the algal lipids), the pyrolysis of algae (*Scenedesmus*) was conducted in a bench-scale fluidized bed fast pyrolysis reactor. Additionally, pyrolysis-GC-MS was performed in order to provide insights into the nature of the primary products obtained from the microalgae pyrolysis. The results from this study have been recently submitted for publication [13].

Materials and Methods

Algae Feedstock: The algae feedstock was dried, ground *Scenedesmus* sp. which had been cultured autotrophically in an open pond. 20 gallons of wet algae (11-16% dry mass) was dried at 60 °C for 24 h. The dried algae clusters (2.9% residual water) were then milled to produce 2 mm particles. The same algae were used for pyrolysis-GC/MS analysis.

Pyrolysis: Pyrolysis was performed at 480 °C and 100 kPa with a 2 s vapor residence time and total run time of 2 h. A screw feeder (Acrison's MD-II Weight Feeder Controller) with an air-locked star rotary valve (Sunco Power Systems) was used as the feeding system and was run at approximately 2.3 kg/h. The feedstock was introduced into the bottom of the draft tube where it contacted the bed material, 60 mesh sand, and was then heated immediately to 480 °C by the bed material for fast pyrolysis. The effluent exiting from the reactor passed through a hot gas cyclone and a ceramic filter (at 450-500 °C) to remove solids (mainly char), and then entered a series of quenching coolers for recovering condensable oil and water. Pyrolysis was performed using 20 lb of dried algae (3% moisture content) which had been ground to a powder (< 2 mm).

After passing the cyclone, four condensers were installed in series to collect bio-oil. The first condenser (C1) was cooled with spouting gas (nitrogen) for heat recovery, the temperature of the gas inside the condenser being measured at 365 °C and 67 °C at the outlet. The second and the third condensers were cooled with tap water and the temperatures were 270 °C and 135 °C, respectively, at their inlets and approximately 10 °C at their outlets. The fourth condenser (C4) used dry ice as a coolant, the temperature at the inlet being approximately 20 °C. After passing through the condensing units, residual gas and vapors were filtered with glass wool which was kept cool with dry ice at -15 °C. The non-condensable gases in the effluent were compressed and reheated to 170 °C and then recycled back into the reactor as fluidizing gas. Oil samples from the reactor walls and final filter were also collected for mass recovery calculations and analysis.

Pyrolysis-GC/MS: pyrolysis GC-MS (Py-GC-MS) was performed using a CDS Analytical Model 5200 Pyroprobe connected to an Agilent 7890 GC with an Agilent 5975C MS detector. Pyrolysis was run in trap mode without the use of a reactant gas and utilized a sorbent tube maintained at 325 °C containing Tenax. Pyrolysis was conducted at 480 °C (1000°C/s heating rate) for 2 s under He using a 1 mg sample packed in a quartz cell and held in place using quartz wool. Each sample was heated to 100 °C in the pyroprobe for 10 s prior to analysis. The valve oven and transfer lines were each set at 325 °C. The column used in the GC was a DB1701 (60m x 0.25mm x 0.25 µm) and the temperature program was as follows: 45 °C for 3 min, followed by a ramp to 280 °C at 4 °C/min with a 10 min hold at the end. The flow rate was set to 1 mL/min using He as the carrier gas and an inlet split ratio of 90:1. The inlet and auxiliary lines were both

maintained at 300 °C and the MS source was set to 69 eV. Py-GC/MS measurements were performed in triplicate for statistical purposes.

Results and Discussion

Bench-scale pyrolysis

Considering first the char product, the ratio of crude oil:char obtained was 3.76 by weight for the oil fractions collected. The char had low calorific content (1970 Btu/lb) and contained 13.3 wt.% volatile matter, while ultimate analysis showed it to contain 15.9 wt. % carbon, together with small amounts of nitrogen (2.3 wt.%), sulfur (0.8 wt.%) and hydrogen (0.8 wt.%). 75 wt.% of the biochar mass was attributed to the presence of ash. SEM images (not shown) indicated that a significant portion of the ash content resulted from the presence of frustules derived from Navicula diatoms that were present in the algae feedstock as a contaminant. The presence of these organisms also explains the high ash content (35.2 wt.%) in the original feedstock. The ash obtained from the biochar consisted of 49.5 wt.% SiO_2, 4.1 wt.% Fe_2O_3, and 11.0 wt.% Al_2O_3 which is consistent with the presence of the silicate frustules [14]. The biochar ash also contained 10.7 wt.% CaO, 1.6 wt.% Na_2O, 5.9 wt.% K_2O, 9.7 wt.% P_2O_5, and 3.1 wt.% SO_3 which were mainly associated with the Scenedesmus sp. (originating from the nutrients supplied to the algae feedstock).

The total oil yield was estimated at approximately 55 wt.%, based on the yield of bio-oil fractions collected and the approximate amount of oil remaining on the reactor walls and piping. Note that this figure is based on the weight of feedstock, excluding its ash content. The filter oil constituted the largest percent of recovered oil product by mass (33.8% of the total), followed by the C3 oil fraction (28.5% of the total, see Table 3). The average density of the oil was 1.1 g/ml, which is slightly lower than that of wood pyrolysis oil [15] but similar to values reported for pyrolysis oil derived from autotrophically grown algae [16,17]. The average total acid number for the oil products was 68 mg KOH/g, which is somewhat lower than typical bio-oil produced from wood pyrolysis [15]. Elemental analysis showed the oil products to contain an average of 27.6 wt.% oxygen, 51.9 wt.% carbon, 9.0 wt.% hydrogen and 8.6 wt.% nitrogen (dry basis), the relatively high nitrogen content being a consequence of the high protein content of the algae. Figure 14 displays the results from ultimate and proximate analyses for several fractions obtained. The lighter oil fractions contained more water and low boiling point compounds than the heavy fractions, although the overall average oxygen and moisture content (~25 wt.%) were typical of lignocellulosic-derived pyrolysis oil.

The results of bomb calorimetry showed the average calorific content of the oil to be approximately 18.4 MJ/kg. This is comparable to bio-oil produced from the fast pyrolysis of wood [14] but is lower than the value of 30 MJ/kg reported by Miao and Wu [16] for pyrolysis oil obtained from fast pyrolysis of Chlorella protothecoides cultured autotrophically. This difference can be attributed to the lower oxygen content (19.43%) of the oil obtained by Miao and Wu (and correspondingly higher carbon and hydrogen contents) as compared to the oil produced in the current study. Additionally, there may also be differences in the water content of the bio-oils (the water content is not reported in references 16 or 17). The reason for these differences in bio-oil properties is not apparent, although we note that Babich et al. [18] reported an intermediate heating value of ~26 MJ/kg for bio-oil obtained from pyrolysis of Chlorella sp. at 450 ºC. The lighter fractions in the current work (C3 and C4) had lower heating values than the heavy fractions due to their higher water content. Simulated distillation GC results, shown in Figure 15, indicated that each fraction contained a high proportion of components boiling in the range for heavy gas oil (343°C-524°C). The lighter fractions also show a significant proportion of products that boil in the range typical of kerosene (204°C-288°C).

Table 3. Product distributions for select oil fractions based on GC-MS analysis.

Compounds (Class of Compounds)	C2 (Area %)	C3 (Area %)	C4 (Area %)	Filter (Area %)
Alkanes	0.0	2.0	0.0	2.6
Alkenes	1.5	8.9	0.0	9.4
Fatty Oxygenates	21.0	12.1	0.0	32.3
Steroids	2.8	0.0	12.9	3.1
Aromatics	0.0	0.0	0.0	1.8
N-containing Compounds	18.7	70.4	86.2	21.7
Unidentified	56.0	6.7	1.0	29.1
Yield of oil fraction (% of total oil recovered)	3.1	28.5	11.4	33.8

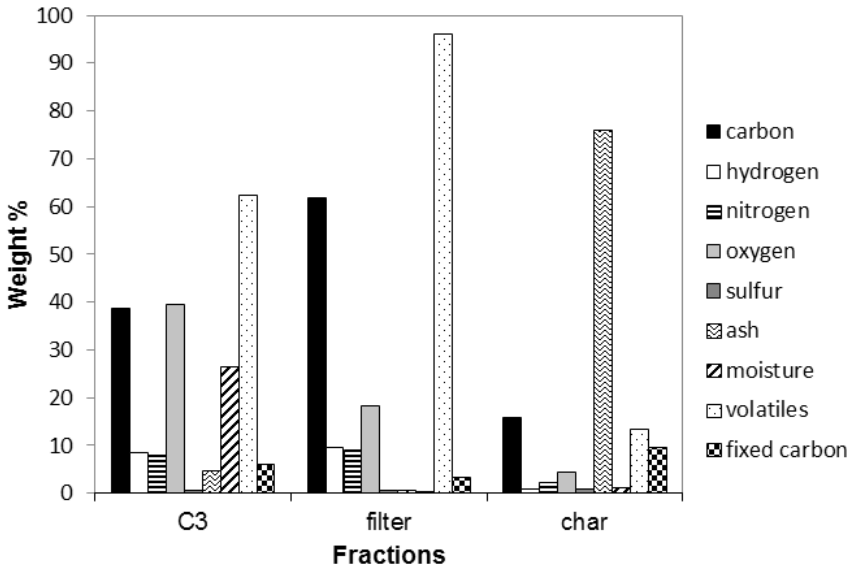

Figure 14. Ultimate and proximate analysis of select fractions obtained from *Scenedesmus* sp.

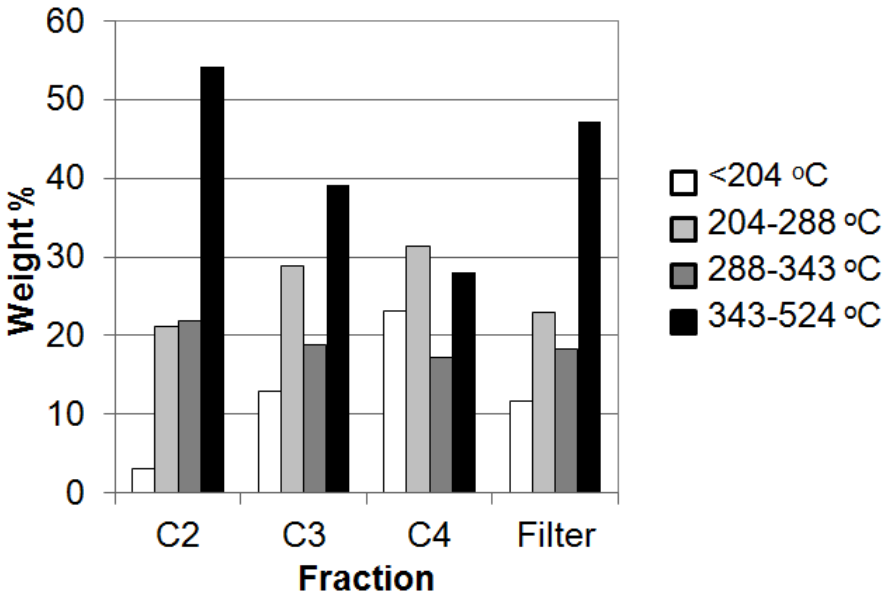

Figure 15. Simulated distillation GC results for select (most abundant) oil fractions.

GC-MS analysis indicated the presence of nitrogenous and oxygenated compounds in the oil fractions such as amides and fatty acids, as well as a variety of hydrocarbons. Many of the compounds were branched or unsaturated as indicated by the C:H ratios and GC-MS results. The area % for the various types of compounds identified for each oil fraction using GC-MS is summarized in Table 3. Nitrogenous compounds identified include amines, amides, pyridines, pyrroles, pyrazoles, pyrazines, nitriles, imidazoles and indoles, although the majority of these compounds were amides. The amides varied in chain length ranging from acetamide to stearamide and also included cyclic amides such as 2-pyrrolidone. Cyclic amides may be formed from protein and amino acid intramolecular cyclization [19-22] whereas linear amides may be formed from primary protein decomposition or from amines in amino acids that reacted with carboxylic acids to produce amides and water (Figure 16). The presence of pyrroles can be attributed to the decomposition of glutamine amino acids present in proteins, as well as decomposed chlorophyll that was present in the algae feedstock [23]. Pyrazines, pyridines, piperidines and pyrazoles are also likely formed from protein decomposition and/or intramolecular cyclization. Imidazoles may be formed from the decomposition of histidine amino acids present in proteins [20] and indoles may be produced from decomposed tryptophan amino acids [21,24]. Each of these compounds may be the result of primary or secondary reactions that occurred during pyrolysis or in the condensed oil phase. Decomposition mechanisms that lead to these products include, but are not limited to: homolytic cleavage, heterolytic cleavage, decarboxylation, decarbonylation, dehydration, deamination, dehydrogenation, condensation and cyclization [22]. While the amount of nitrogenous compounds formed seems high, the results agree with elemental analysis. For example, if the average nitrogenous compound is compositionally similar to octanamide, then based on its empirical formula, a nitrogen content of 10 wt. % would be expected. Since N-containing species constituted less than 100% of the various oil fractions, a nitrogen content of less than 10 wt. % is to be expected.

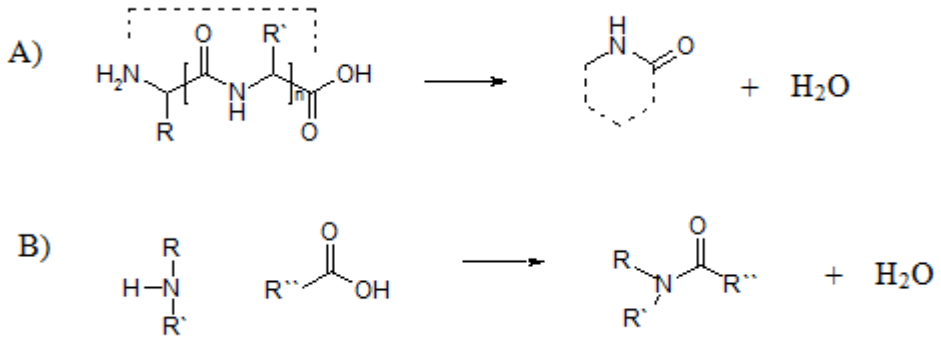

Figure 16. A) Intramolecular cyclization of proteins resulting in pyrrolidone structures. B) Carboxylic acids react with amines to produce linear amides.

Fatty oxygenates identified include aldehydes, ketones, acids, and alcohols with long carbon chains, including saturated and unsaturated, branched and linear isomers. Alkanes and alkenes in the products were identified in accordance with retention time calibrations and mass spectra analysis based on a NIST library. The majority of these hydrocarbon compounds were formed primarily from the pyrolysis of the lipid fraction (triglycerides and fatty acids) of the algae feedstock. Lipid pyrolysis mechanisms are complex and have been thoroughly investigated [25-31]. Steroids and aromatic compounds such as phenols, naphthalene and toluene were also observed in the oil products, particularly in the filter oil.

Pyrolysis-GC-MS

The pyrogram displayed in Figure 17 shows that pyrolysis of *Scenedesmus* sp. at 480 °C produces a significant amount of fatty oxygenates which appear at various retention times in the pyrogram, particularly beyond 28 min. These compounds, which include alcohols, ketones, acids and aldehydes, are derived predominantly from the pyrolysis of the fatty acids and triglycerides present in the algae. Although many of these peaks could not be not unambiguously identified, the peak obtained at 44.1 minutes corresponds to phytol, which would derive from chlorophyll [23]. The pyrogram also shows that a large amount of nitrogenous products are created; the majority of these products appear to be amines such as pyrroles and piperidines based on comparison of spectra with the NIST database, whereas the nitrogenous compounds from previous reactions in a fluidized bed reactor appear to be mostly amides. The pyrolysis conditions may have been more severe in the fixed bed reactor such that they underwent secondary reactions to produce the observed amides, or, more likely, secondary reactions may have occurred in the bio-oil (i.e., $RCOOH + RNH_2 \rightarrow RCONHR + H_2O$). Also, pyrazines were much more abundant in the bio-oil from the fixed bed reaction than in the products seen from the Py-GC/MS of the algae. Pyrazine production can occur as the result of a sequence of reactions following the Maillard reaction between sugars and proteins in the algae [32]. Since the pyrolysis vapors generated in the pyroprobe were quickly swept to the GC inlet they were not able to undergo many of the secondary reactions that may occur in condensed bio-oil to produce pyrazine derivatives.

The pyrogram also contains peaks corresponding to fatty olefins, paraffins, and aromatic compounds which are also likely produced from the pyrolysis of the lipid fraction of the algae. Carbohydrate pyrolysates such as butyrolactone and furan derivatives were observed in small quantities in the oil fractions from the fluidized bed reactor but are more abundant in the pyrogram shown in Figure 17. This implies that they are primary pyrolysis products which can

undergo secondary reactions, thereby explaining why there is a lower abundance of these compounds in the condensed pyrolysis oil.

The area % for various types of compounds seen in the pyrogram is shown in Table 4. The majority of the peaks can be attributed to carbohydrate pyrolysates, fatty oxygenates, aromatics and nitrogen-containing compounds, with smaller amounts of alkanes and alkenes being present. The Py-GC/MS results for product distributions agree to a certain extent with the GC-MS results obtained from the fluidized bed bio-oil fractions when considering the weight distributions for each of the oil fractions. However, the Py-GC/MS analysis did not detect the presence of steroids which may have condensed in the transfer line prior to the GC inlet. In addition, GC-MS analysis of the oil fractions appeared to show higher percentages of nitrogen-containing compounds than the Py-GC/MS analysis because fewer of the fatty oxygenated hydrocarbons were detected. This is likely the result of secondary reactions that occurred during pyrolysis or in the oil during condensation. The Py-GC/MS analysis was also able to detect more carbohydrate pyrolysates which did not appear in GC-MS analysis of the bio-oil fractions. However, both techniques indicate that the major components of pyrolysis oil produced from *Scenedesmus* algae are fatty oxygenated hydrocarbons and nitrogen-containing molecules such as amides and amines.

Table 4. Distribution of product types generated from *Scenedesmus* sp. pyrolysis in a pyroprobe at 480 °C.

Compounds	Area % (standard deviation)
Alkanes	2.4 (0.8)
Alkenes	2.1 (0.9)
Fatty Oxygenates	23.7 (1.6)
Aromatics	8.9 (1.6)
N-containing compounds	14.3 (1.6)
Carbohydrate pyrolysates	8.6 (0.63)
Unidentified	40.0 (3.7)

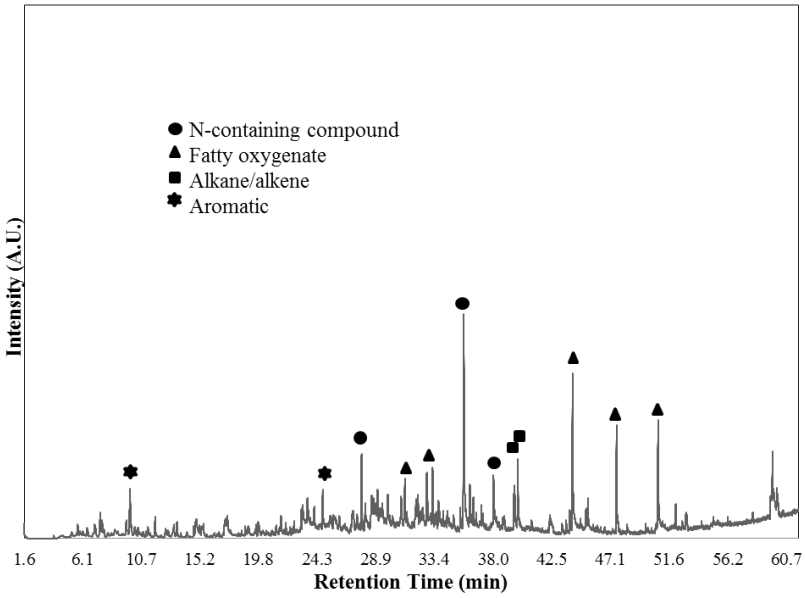

Figure 17. Pyrogram displaying products formed from *Scenedesmus* sp. pyrolysis in a pyroprobe at 480 °C.

Conclusions

Two reactor scales were utilized in order to compare and understand the origin and the formation of products from fast pyrolysis of *Scenedesmus* algae. Thorough analysis of the oil products from the fluidizing unit was performed in order to gain an understanding of the composition and property of the oils. First, a technical, larger scale production of bio-oil from the fast pyrolysis of a dried microalgae feedstock was investigated using a fluidized bed reactor. Product analysis shows the various fractions of the bio-oil collected are, in certain respects, comparable to pyrolysis products from lignocellulosic feedstocks. Indeed, the overall heating value of the oil product is typical of lignocellulose-derived pyrolysis oil, although the average total acid number of the oil is lower than for bio-oil produced from wood pyrolysis. Furthermore, the bio-oil has a higher average nitrogen content due to the high protein content of the algae feedstock. Micro-scale Py-GC-MS was also used to characterize products formed from pyrolysis of the dried *Scenedesmus* sp. in order to establish a more fundamental understanding of the origin of the various pyrolysates, as well as test whether the products formed on a small scale were comparable to a larger scale fluidizing unit. Large amounts of fatty oxygenates and nitrogenous products were observed from the pyrolysis of the algae, while the Py-GC-MS was able to detect significant production of carbohydrate pyrolysates which were observed in only very minor amounts in the fluidized bed pyrolysis oil fractions. Differences observed in the products generated from the different reactors may be due to secondary reactions that could have occurred during pyrolysis in the fluidized bed or in the oil during condensation.

2.4.3. Lipid extraction

Introduction

Microalgae possess attributes such as high growth rate and high lipid production that make them particularly suitable for the production of fuel [33]. Lipid production and the lipid extraction process are important factors that need to be thoroughly understood in order to convert algae-derived lipids into useful fuels and chemicals. The purpose of this investigation was to test three literature methods for the extraction of lipids from algae. Three solvents of key interest are chloroform/methanol, hexanes/isopropyl alcohol, and pure hexanes. The chloroform/methanol method has, in the past, been widely used to extract lipids from algae but, prior to this work, its effectiveness and the rate of lipid extraction had yet to be proven for *Scenedesmus* sp. algae.

Materials and Methods

Microalgae Cultivation and Preparation: Oven-dried *Scenedesmus dimorphus* algae (3% water content) which had been cultivated in a photobioreactor were ground in a coffee grinder to a particle size of less than 1 mm. After grinding and before all extractions, the algae was heated to 100 ^{0}C for 20 min to remove residual water. All extraction experiments were performed in triplicate for statistical purposes.

Lipid Extraction using Chloroform and Methanol: Lipids were extracted from the *Scenedesmus* algae using a mixture of chloroform-methanol-deionized water (2:2:1) according to the Bligh and Dyer method [34]. For every 10 g of algae used, 200 ml of chloroform, 200 ml methanol, and 100 ml of deionized water were used. After placing 10 g of algae in an Erlenmeyer flask, 100 ml chloroform and 200 ml methanol were added to the flask. The mixture was then shaken for 10 min, after which an additional 100 ml chloroform and 100 ml deionized water were added. This mixture was then shaken for 110 min. The mixture was then immediately filtered to remove the algae so as avoid any further extraction of lipids. Afterwards, the mixture was transferred to a separatory funnel to allow separation of the organic and aqueous layers. Using a rotary

evaporator, the chloroform was evaporated and the weight of the extracted lipids was recorded. This experiment was then repeated in an effort to determine the amount of lipid extracted at different times. In this case the solvents were added to the algae at one time. 4 ml samples were then taken from the mixture over a 2 h time period at intervals of 5, 10, 15, 30, 45, 60, 90 and 120 min. Each sample was immediately filtered right after being taken to remove any algae remaining. The chloroform layer was then separated from the methanol and deionized water layer and was analyzed using an Agilent 7890 gas chromatograph (GC) for boiling point distribution. The method performed followed ASTM D2887.

Lipid Extraction using Hexanes and Isopropanol: Lipids were extracted from *Scenedesmus* algae using a mixture of hexanes and isopropyl alcohol (3:2). For every 10 g of algae used, 108 ml of hexanes and 72 ml of isopropyl alcohol (IPA) were used. This ratio is based on the extraction method used by Hara and Radin [35]. After placing 10 g of algae in an Erlenmeyer flask, 108 ml of hexanes and 72 ml of isopropyl alcohol were poured into the flask. The mixture was then shaken for 120 min. After shaking was complete, the mixture was immediately filtered to stop the extraction of lipids from proceeding. The mixture was then transferred into a separatory funnel. 5 g of sodium sulfate and 75 ml of deionized water were then added to the mixture to create a separation of layers. Removal of the hexanes/lipid layer from the funnel and rotary evaporation of the hexanes then followed. The weight of the lipid extracted was determined gravimetrically. This experiment was then repeated in an effort to determine the rate at which the lipid was extracted. 4 ml samples were taken over a 2 h time period at intervals of 5, 10, 15, 30, 45, 60, 90 and 120 min. Each sample was immediately filtered after being taken to remove any remaining algae. The hexanes layer was then separated from the isopropyl alcohol layer and was analyzed by GC according to ASTM D2887.

Lipid Extraction using Pure Hexanes: Lipids were extracted from *Scenedesmus* algae using only hexanes. For every 10 g of algae used, 180 ml of hexanes was used. After placing 10 g of algae in an Erlenmeyer flask, 180 ml of hexanes was added to the flask and then shaken for 120 min. Immediately after shaking, the mixture was filtered to remove any remaining algae. Next, the hexanes were removed on a rotary evaporator, leaving behind only the extracted lipids. Determination of the weight of the extracted lipids concluded the extraction. This experiment was then repeated in an effort to determine the rate of extraction of the lipids. 4 ml samples were taken over a 2 h time period at intervals of 5, 10, 15, 30, 45, 60, 90 and 120 min. In each case the samples were filtered to remove any remaining algae and were then analyzed by GC according to ASTM D2887.

Results and Discussion

Chloroform-Methanol Lipid Extraction: As seen in Table 5, the chloroform/methanol extraction method yielded an average of 15.1 wt % extracted lipids after a 2 h extraction time. Overall, this method extracted the largest amount of lipid. This may to be due to the polarity of the chemicals used and preferential solubility of the lipids extracted. The lipids were soluble in the chloroform (organic layer) which had intermediate polarity whereas the algae remained behind in the polar, aqueous layer. According to literature for the Bligh and Dyer method, which is considered to be the benchmark for all lipid extractions, maximum lipid extraction occurs within the first 10 minutes [28]. However, Figure 18 shows that for the *Scenedesmus* algae used in this work maximum lipid extraction occurs around the 90 minute mark.

Hexanes-Isopropanol Lipid Extractions: As seen in Table 5, the hexanes/isopropyl alcohol method yielded an average of 5.0 wt % extracted lipids after a 2 h extraction time. The hexanes/isopropyl extraction incorporated a polar and non-polar solvent and the non-polar solvent (organic layer) was analyzed for lipid content. Hence, the lipids may have had limited

solubility in this fraction. In regards to the extraction rate, Figure 19 shows that maximum lipid extraction occurs approximately 90 min after starting the extraction. This is consistent with the extraction rate of the chloroform/methanol method.

Pure Hexanes Lipid Extractions: As seen in Table 5, the pure hexanes extraction method yielded an average of 5.0 wt % extracted lipids after a 2 h extraction time. Since this method only has a non-polar component and no polar component, it makes sense that the wt % extracted is less than that of the chloroform/methanol method. This method seems to produce the same results as that of the hexanes/isopropyl alcohol method, indicating that the isopropyl alcohol had negligible effect on the extraction. Figure 20 shows that maximum extraction occurs around the 15 minute mark for a single extraction but reproducibility for this method was inconsistent. The results lack precision possibly due to inhomogeneity in extraction sampling, differential solubility of products, or solvent evaporation post sampling.

Table 5. Results from 2 h lipid extraction experiments.

Extraction solvent	Time	Wt% lipids extracted
Chloroform-methanol	2 h	15.1
Hexanes-IPA	2 h	5.0
Hexanes	2 h	5.0

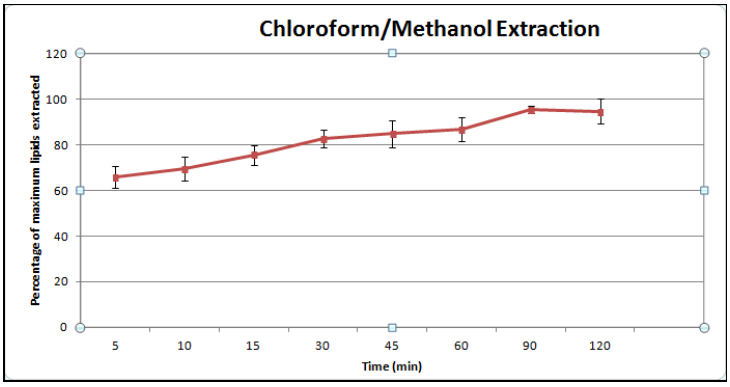

Figure 18. Extraction of lipids over time using chloroform/methanol.

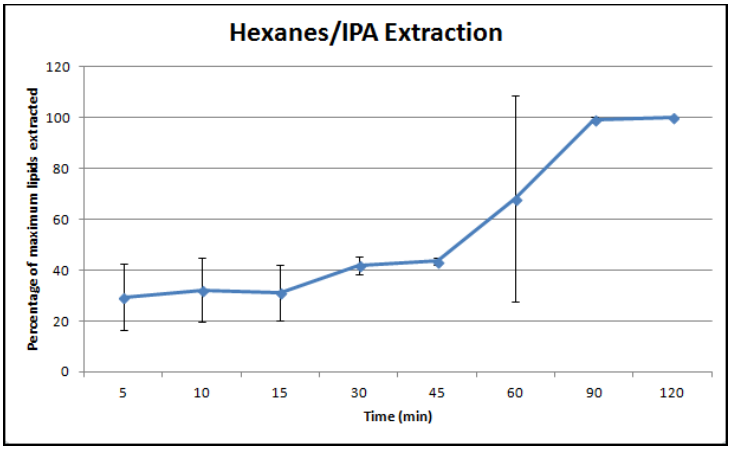

Figure 19. Extraction of lipids over time using hexanes/isopropyl alcohol.

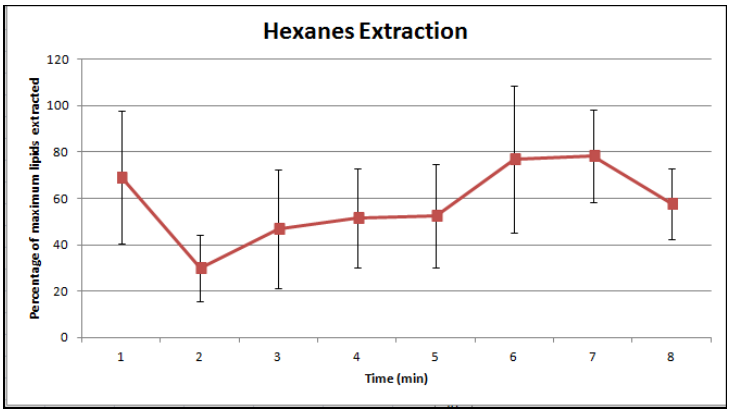

Figure 20. Extraction of lipids over time using pure hexanes.

Conclusions

Overall, it was determined that the pure hexanes extraction method only yielded a maximum of 5 wt% extracted lipids after 2 h extraction time. This is the same as the extraction method using hexanes/isopropyl alcohol which also extracted about 5 wt% lipids after 2 h. In contrast, the chloroform/methanol extraction method yielded 15 wt% lipids over a 2 h period. On-going studies in this area are focused on the use of supercritical solvents for lipid extraction (hexane, CO_2), as well as the development of solvent systems for lipid extraction from wet algae.

2.4.4. Lipid upgrading to hydrocarbons

Introduction

A number of problems associated with the high oxygen content of biodiesel have caused attention to shift towards the catalytic deoxygenation of lipids for the production of fuel-like hydrocarbons, hydrodeoxygenation *via* hydrotreating being the most developed route. Unfortunately, this approach requires high pressures of H_2 and sulfided catalysts that risk contaminating the products with sulfur. An alternative lies in the deoxygenation of lipids *via* decarboxylation/decarbonylation ($deCO_x$), which proceeds under considerably lower H_2 pressures and over simple metal catalysts. Notably, lipids from inedible and high yield biomass sources (tall oil and microalgae oil) have been successfully converted to hydrocarbons *via* $deCO_x$, illustrating that this technology can be employed to produce second-generation biofuels. However, most work has focused on the use of costly Pd or Pt dispersed on carbon, catalysts that – once spent – cannot be regenerated by the combustion of the carbonaceous deposits that cause catalyst deactivation. Through our work, we have shown that inexpensive Ni dispersed on oxidic supports – the performance of which can rival that of precious metal catalysts – can be easily regenerated by calcination. Furthermore, the effect of the H_2 partial pressure and catalyst acidity on catalyst performance and deactivation has been investigated, a reaction scheme has been proposed and the potential of the products as transportation fuels has been evaluated.

Experimental

Catalyst preparation and characterization

The Layered Double Hydroxide (LDH) catalysts and the supported metal catalysts used in our work were prepared *via* precipitation and impregnation, respectively, using materials and procedures the description of which can be found elsewhere . The surface area, pore volume and average pore radius of the catalysts were determined via N_2 physisorption. Powder X-ray diffraction (XRD) measurements were performed in order to determine the average crystallite size of the LDH and the average metal particle size of both catalysts. The reducibility of the catalysts in this study was investigated via temperature programmed reduction (TPR) and the Ni

metal specific surface area was measured by means of H_2 chemisorption. The acidity and the basicity of the catalysts were assessed through the temperature programmed desorption (TPD) of NH_3 and CO_2, respectively. The description of the instrumentation and methods employed in the aforementioned tests has been reported . The nature and the amount of the carbonaceous deposits on the surface of spent catalysts was studied by means of TGA performed under flowing air (50 ml min^{-1}) on a TA instruments Q500 thermogravimetric analyzer. The temperature was ramped from room temperature to 800 ºC at a rate of 10 ºC/min.

Catalyst testing in the deoxygenation of fatty acids and triglycerides via deCO_x

Stearic acid (97%) was purchased from Acros Organics and analyzed by means of GC. This analysis showed the sample to be ~99.5% stearic acid and ~0.5% palmitic acid. Tristearin (95%) was purchased from City Chemical and analyzed using instruments and methods which have been reported, along with the results of the analysis [36,38]. Experiments were performed in a mechanically stirred 100 mL stainless steel autoclave operated in batch [36,37] or semi-batch mode. Typically, the catalyst (0.5 g) in powder form (particle size <150 μm) was reduced *in situ* at 350 °C under flowing 10% H_2/N_2 for 3 h prior to purging the reactor with Ar and adding both solvent (dodecane, 25 g) and feedstock (1.75 g). The autoclave was then purged three times with Ar prior to being pressurized with the required gas (N_2, 10 % H_2/N_2 or H_2) and heated to the reaction temperature. The system was kept at 300±2 °C and 135 psi for 1.5 h or at 355±5 ºC and 580 psi for 6 h in deoxygenation experiments involving stearic acid and tristearin, respectively. The autoclave temperature was measured by a type-K Omega thermocouple placed inside the reactor body. The reactions were performed under mechanical stirring of 1,000 rpm (and under constant gas flow of 70 mL/min in the case of semi-batch reactions). Volatile products were collected from the gas stream leaving the reactor by cooling the latter with a condenser kept at room temperature prior to venting. At the completion of each test, forced air and an ice bath were sequentially used to facilitate cooling. Once the reactor reached room temperature, the system was slowly depressurized. Oil and catalyst were removed from the reactor and separated by gravity filtration to isolate the product. The catalyst was then washed twice with chloroform to yield additional material.

Product analysis

Prior to chromatographic analysis, samples were diluted with chloroform, typically in a 1:10 weight ratio. Simulated distillation-GC analyses were performed according to ASTM D2887, using an Agilent 7890 GC equipped with a MultiMode inlet and a J&W Scientific D-2887 capillary column. The heterogeneous nature of the catalyzed reactions was confirmed by analyzing representative liquid products for either Ni or Pd in solution *via* Inductively Coupled Plasma – Atomic Emission Spectroscopy. These leaching studies revealed <7 ppm of Ni and ~0.5 ppm of Pd in the liquid products (regardless of the feed and the H_2 partial pressure employed), which indicates that the reactions are not catalyzed homogeneously by metals leached into solution.

Results & Discussion

Initial studies in a batch reactor under inert atmosphere using carbon-supported Pt, Pd and Ni catalysts

At the beginning of this project, a significant body of data pointed to the viability of hydrocarbon production via the proposed metal-catalyzed deoxygenation of vegetable oils and animal fats. For example, the gas phase selective decarboxylation of carboxylic acids had been studied over nickel and palladium catalysts , while the production of linear olefins from saturated fatty acids and fatty acid esters had also been achieved using nickel catalysts . Murzin and co-workers had also reported the results of detailed studies they had performed on the metal-catalyzed

deoxygenation of fatty acids (and fatty acid methyl and ethyl esters) over a variety of catalysts. These workers found palladium supported on activated carbon to be a particularly effective catalyst for this purpose. In addition, Do et al. had also reported that Pt/Al_2O_3 is an effective catalyst for the deoxygenation of fatty acid methyl esters.

Inspired by these reports, initial studies were performed in our laboratory to confirm the suitability of metal-catalyzed deoxygenation for the production of hydrocarbon fuels from triglycerides. As for the deoxygenation of fatty acids and their simple alkyl esters, deoxygenation of the triglyceride is in principle accomplished via removal of the carboxyl group in the fatty acid structure as carbon dioxide and/or carbon monoxide, thereby producing linear hydrocarbons. Additional cracking of the fatty acid chain may occur, resulting in the formation of hydrocarbons spanning a range of carbon chain lengths. Following on from Murzin's reports which concluded that precious metal catalysts (particularly Pd) are active for the decarboxylation of fatty acids and their methyl esters, we studied the upgrading (deoxygenation) of model triglyceride compounds, such as tristearin (glycerol tristearate) and triolein (glycerol trioleate) over Pd, Pt and Ni catalysts and extended this work to include salad oil (a refined soybean oil). Promising results were obtained: at 350 °C, the foregoing feedstocks were converted to aliphatic hydrocarbons in the range C5-C17 with a yield of up to 70 wt% based on the total liquid, oxygen being rejected as a mixture of CO_2 and CO. The remaining part of the liquid product consisted of heavy hydrocarbons and oxygenates. Also encouraging was the fact that the performance of the Ni catalysts developed in our laboratory generally meets or exceeds that of the considerably more expensive Pd or Pt catalysts. Typical results for the deoxygenation of tristearin and soybean oil over 20% Ni/C under a nitrogen atmosphere in a batch reactor are given in Figs. 21 and 22, respectively.

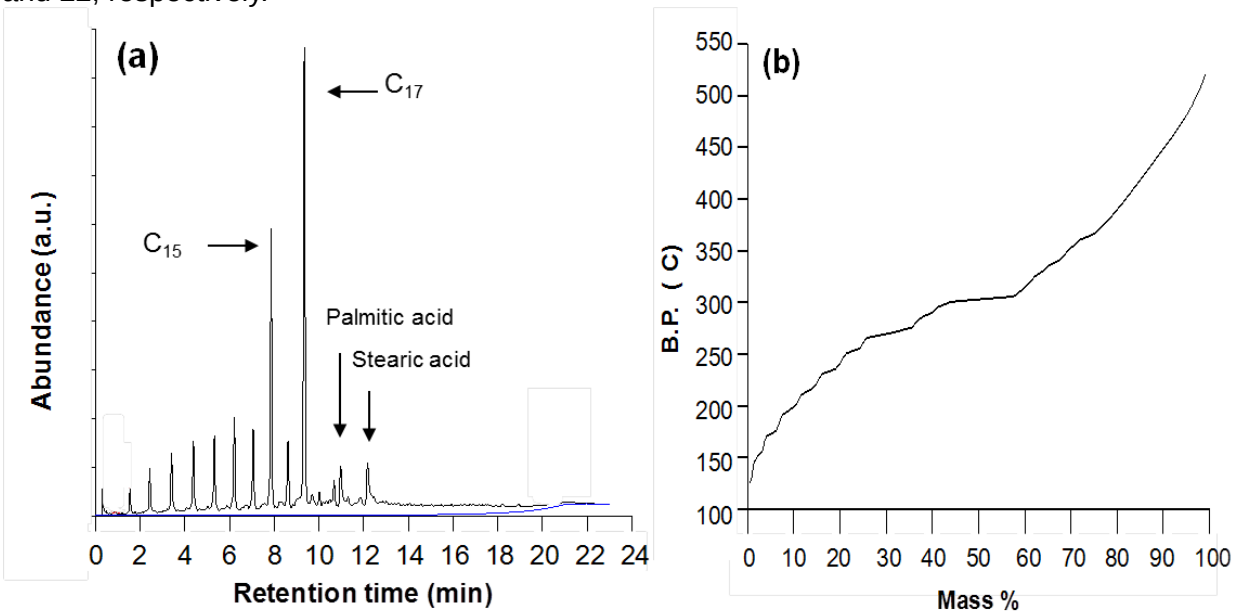

Fig. 21. Results of simulated distillation GC performed on product obtained from tristearin deoxygenation over 20 wt% Ni/C: (a) gas chromatogram, (b) boiling point distribution plot.

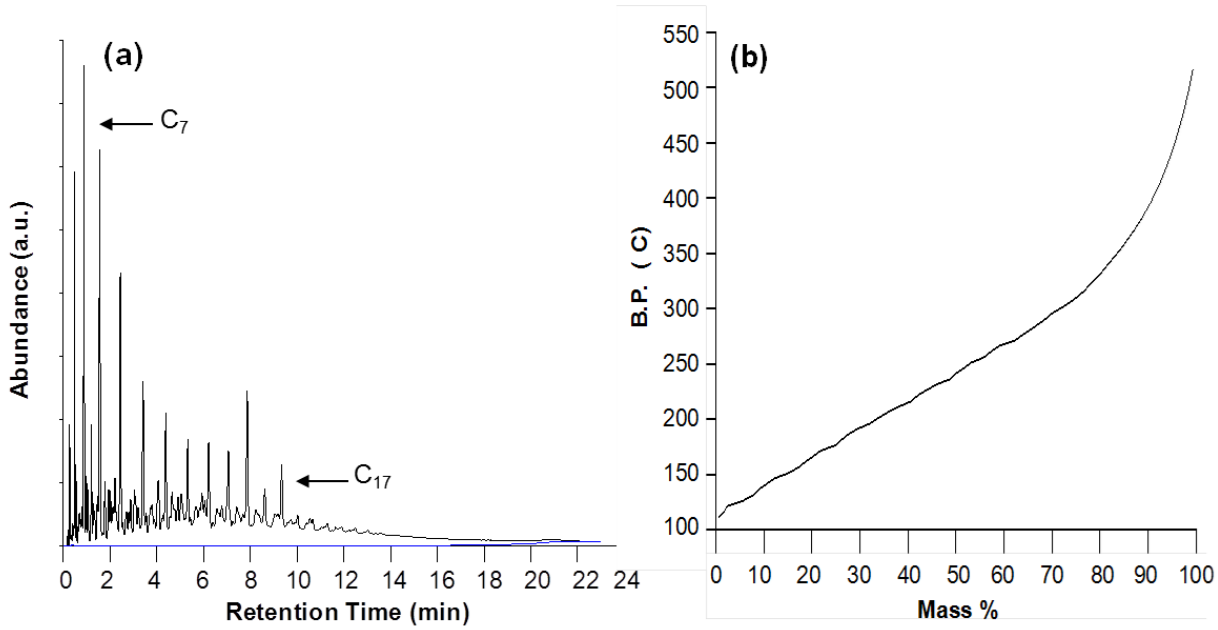

Fig. 22. Results of simulated distillation GC performed on product obtained from soybean oil deoxygenation over 20 wt% Ni/C: (a) gas chromatogram, (b) boiling point distribution plot.

As shown in Fig. 21a, simulated distillation gas chromatography reveals the presence of C7-C17 linear alkanes in the liquid product obtained from tristearin deoxygenation, with *n*-heptadecane and *n*-pentadecane being particularly abundant. Also detected are palmitic and stearic acid, which in separate experiments have been identified as reaction intermediates. The corresponding boiling point distribution plot for the liquid product is shown in Fig. 3b. The plateau at ca. 300 °C corresponds to *n*-heptadecane, while ca. 40 wt% of the liquid boils at a temperature in excess of this. In an effort to identify the high boiling compounds present, the liquid was subjected to additional analysis by GC-MS and ^{13}C NMR spectroscopy. According to GC-MS data, the high boiling components consist of palmitic and stearic acids (b.p. 351-352 and 383 °C, respectively), together with small amounts of linear hydrocarbons (mainly alkanes) falling in the range C18-C35, and a number of unidentified compounds. Based on the work of Do et al. , heavy oxygenates (>C18) are likely to result from condensation reactions such as ketonization and transesterification; subsequent deoxygenation of these oxygenates via reduction or CO/CO_2 expulsion would then give rise to the observed higher alkanes.

In the case of soybean oil, the liquid product consists predominantly of hydrocarbons in the C6-C10 range (Fig. 22a). Compared to tristearin, the selectivity to light hydrocarbons (≤ C10) is increased, reflecting the greater reactivity of the unsaturated fatty acid chains towards cracking. Furthermore, although these hydrocarbons mainly correspond to linear alkanes, the presence of other hydrocarbon species is suggested by the many smaller signals present in the chromatogram. This was confirmed by ^{13}C NMR spectroscopy (data not shown), the presence of internal olefinic carbons (multiple signals at 122-130 ppm) being indicated. Signals corresponding to terminal olefins (ca. 114 and 139 ppm) were not observed. Fig. 22b shows the boiling point distribution plot corresponding to the chromatogram in Fig. 22a. This indicates that ca. 65 wt% of the liquid product boils in the 150-300 ºC range, which corresponds roughly to the boiling range of aviation fuel.

In short, in our initial work – which was published in the journal Topics in Catalysis – the metal-catalyzed deoxygenation in the absence of hydrogen was found to be an effective method for the conversion of triglycerides to liquid hydrocarbons. The distribution of carbon chain lengths in the product was found to be strongly influenced by the degree of unsaturation of the constituent fatty acid chains in the triglycerides and by the nature of the catalyst. Moreover, the selectivity to light hydrocarbons was observed to increase with increasing unsaturation of the triglyceride, reflecting the greater reactivity of the unsaturated fatty acid chains towards cracking. Compared to Ni, catalysts containing Pd or Pt supported on activated carbon show lower activity for both cracking of the fatty acid chains and for triglyceride deoxygenation.

Uncatalyzed reactions performed in a fixed-bed reactor

A this point, efforts were focused on the study of uncatalyzed reactions in order to ascertain the contribution of thermal reactions to subsequent catalyzed experiments. Experiments were conducted at 300 psig in a fixed-bed reactor (9 mm x 100 mm, d x l). The reactor bed was packed with glass beads of 1 mm average diameter. Nitrogen was used as the carrier gas at a flow rate of 30 ml/min (STP). Soybean oil (SBO) was fed to the reactor at 10.64 g/h, giving a nominal LHSV of 1 h^{-1}. Tables 6 and 7 show the conversion of SBO and the yields of the main fractions in the liquid product for experiments conducted at different temperatures under both atmospheric pressure and 300 psig pressure. The conversion was estimated based on the total yield of the product obtained, i.e., conversion = 100 x (weight of liquid product + gas + coke)/weight of feed, where weight of liquid product = product fraction (BP<375 °C) x total weight of liquid recovered. Note that for the purposes of this calculation, all of the liquid components boiling above 375 °C are considered to be starting material (SBO), while everything below this cut point is considered product. The diesel-like fraction is defined to be the components from C10 to C18 with boiling point from 177 °C to 325 °C, while C17 and C18 are defined to be the fractions with boiling points ranging from 295 °C – 314 °C and 314 °C – 325 °C, respectively. Likewise, palmitic acid is assumed to be the fraction with boiling point from 330 °C to 341°C and stearic acid to be the fraction with boiling point from 352 °C to 368 °C.

Table 6. Conversion of soybean oil (SBO) and product yields from thermal cracking under atmospheric pressure

Temperature (°C)	Conversion (%)[a]	Yield (% of liquid product)				
		Diesel-like fraction	C17	C18	Palmitic acid	Stearic acid
350	15	7.3	0.6	0.4	2.3	4
375	33	10.4	1.4	0.5	4.6	15
400	51	15.1	3.0	1.0	5.9	15.5
450	65	29	5.4	2.0	8	17
500	67	33.4	5.4	2.0	7.1	16

[a] Conversion = 100 x (weight of liquid product + gas + coke)/weight of feed, where weight of liquid product = product fraction (BP<375°C) x total weight of liquid recovered.

Table 7. Conversion of SBO and product yields from thermal cracking under 300 psig pressure

Temperature (°C)	Conversion (%)	Yield (% of liquid product)				
		Diesel-like fraction	C17	C18	Palmitic acid	Stearic acid
350	19	7.3	0.9	0.4	2.8	4
375	29	8.4	1.4	0.5	4.6	9
400	61	20.9	4.3	1.3	7.4	23
450	73	46.6	9.0	2.8	5.6	5
500	74	54.1	7.0	2.6	3.3	3

As shown in Figure 23, the conversion of SBO increased from 16 wt% to 67 wt% when the cracking temperature was increased from 350 °C to 500 °C at atmospheric pressure. Correspondingly, the SBO conversion can reach more than 80 wt% at 500 °C under 300 psig pressure. Indeed, the conversion of SBO is higher under 300 psig pressure than under atmospheric pressure at all cracking temperatures except at 375 °C. Interestingly, the yields of a number of the components (C17, C18, palmitic acid and stearic acid) increase with cracking temperature initially and then decrease when the cracking temperature is above 400 °C or 450 °C. In the case of stearic and palmitic acid, these data suggest that the acids undergo decarboxylation at high temperatures to afford hydrocarbons (C17 and C15, respectively).

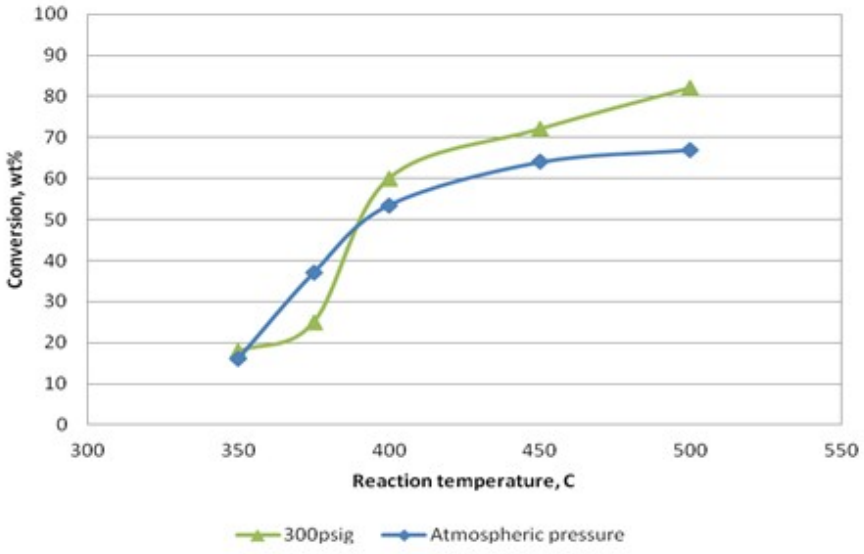

Figure 23. Effect of reaction pressure on the conversion of SBO at the different cracking temperatures

Figure 24 and 25 show the yields of the total liquid product and the diesel-like fraction as a function of temperature for the thermal cracking of SBO at atmospheric pressure and 300 psig, respectively. In both cases, the yield of total liquid product decreases with increasing cracking temperature. Figure 24 shows that the yield of the diesel-like fraction (i.e., total liquid yield x % diesel-like fraction in liquid) initially increases with the cracking temperature, until it approaches *ca*. 30 wt% at 500 °C under atmospheric pressure. Under 300 psig the yield of the diesel-like

fraction reaches 37 wt% at 450 °C, but then decreases to 34 wt% at 500 °C because the amount of liquid product drops significantly. A comparison of Figures 24 and 25 shows that the yields of the diesel-like fraction obtained at 300 psig are higher than those obtained at atmosperic pressure.

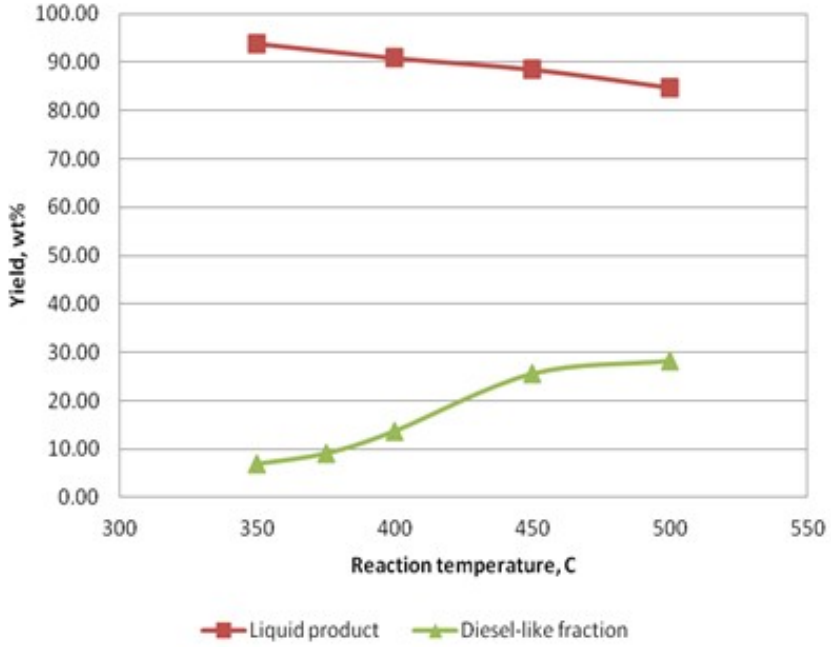

Figure 24. Yields of liquid product and diesel-like fraction obtained from thermal cracking of SBO at atmospheric pressure

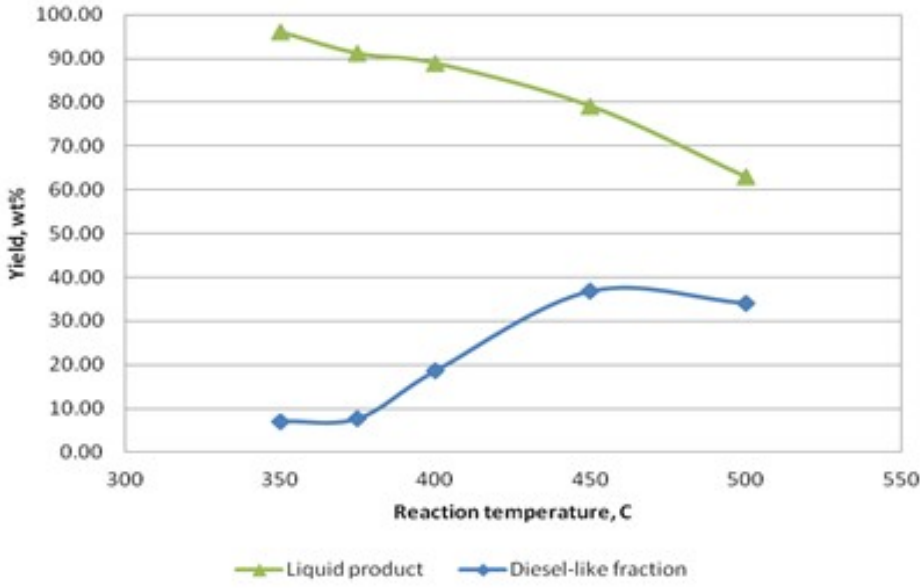

Figure 25. Yields of liquid product and diesel-like fraction obtained from thermal cracking of SBO at 300 psig

Overall, these results show that the production of diesel-like product is favored by high reaction pressures and by temperatures in the range 450-500 ºC; however, yields are fairly modest.

Consequently, subsequent efforts were refocused on catalytic decarboxylation, using semi-batch and fixed bed reactors.

Studies in a batch reactor under inert atmosphere using Ni-based catalysts
Encouraged by the promising results obtained in our laboratory over carbon-supported Ni, the deoxygenation of triolein and soybean oil under nitrogen atmosphere was investigated using a batch reactor over Ni-Al, Ni-Mg-Al and Mg-Al layered double hydroxides, as well as 20 wt.% Ni/Al_2O_3. The results of these experiments are shown in Table 8.

Table 8. Percent conversion of triolein and soybean oil to hydrocarbons obtained from deoxygenation experiments[a,b]

Experiment	Conversion (%)	C1-C7 Yield (%)	C8-C17 Yield (%)	C18 Yield (%)
Triolein				
No catalyst	6	0.2	1.7	91.0
Ni-Al	91	5.4	42.6	36.1
Ni-Mg-Al	73	4.5	50.5	30.5
Mg-Al	76	5.1	49.6	33.5
Ni/Al_2O_3	70	4.1	46.8	40.4
Soybean oil				
No catalyst	16	0.7	23.8	62.3
Ni-Al	74	7.5	52.9	19.1
Ni-Mg-Al	49	1.3	29.0	54.1
Mg-Al	72	5.6	47.8	25.4
Ni/Al_2O_3	68	3.2	46.3	51.2
Recycled Ni-Al	67	7.7	54.4	21.1

[a]%Conversion = 100×(mmol CO + CO_2 + O_2 + CH_4 formed)/3×(mmol triglyceride used).
[b]Yield = 100×(wt. of hydrocarbon fraction/total wt. of solid + liquid + gaseous products).

According to the analysis of the gaseous products (not shown) deoxygenation was found to proceed via removal of the carboxyl group in the fatty acid structure as CO_2 and CO, while according to the analysis of the liquid products (shown in Table 8) additional cracking of the fatty acid chains resulted in the formation of mainly liquid (C5–C17) hydrocarbons. In comparison with triolein, the greater unsaturation of soybean oil resulted in increased cracking, leading to the formation of lighter hydrocarbons and higher amounts of coke deposits.

The fact that in this particular set of experiments the catalysts employed did not comprise carbon as the support allowed for the spent catalysts to be studied by means of thermogravimetric analysis (TGA) in air. Figure 26 shows the results of TGA in air performed on the Ni-Al catalyst used for soybean oil deoxygenation. The derivative weight loss profile shows one main, broad peak at 550 °C which can be attributed to coke.

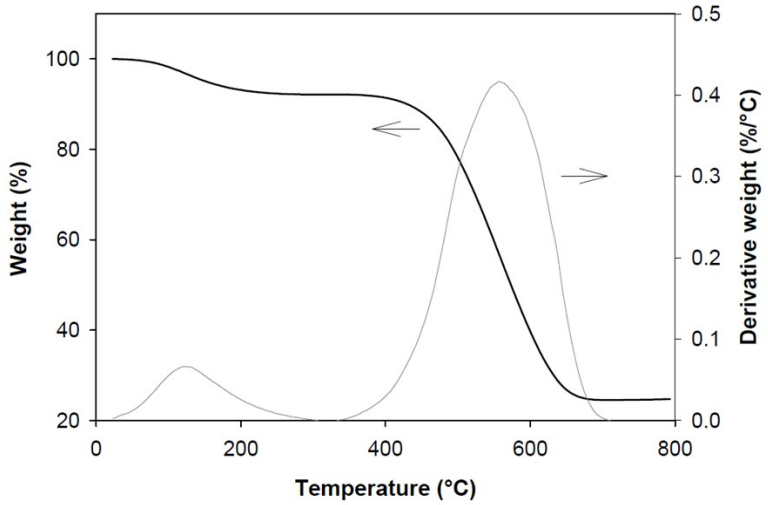

Figure 26. Thermogravimetric analysis in air of Ni-Al catalyst used for soybean oil deoxygenation.

In order to assess the effect of solid formation on catalyst activity, recycle experiments were performed. Representative data are shown in Table 8 for spent Ni-Al LDH catalyst in soybean oil deoxygenation. Between runs the catalyst was washed with $CHCl_3$ at room temperature and dried in a vacuum oven at 80 °C. Upon reuse, decreased activity was observed, as reflected in a decrease in soybean oil conversion from 74% to 67%. Given that metal leaching was determined to be negligible, this loss in activity cannot be attributed to the loss of active components to the reaction medium. Instead, it is likely being caused by coke formation.

The progress of soybean oil deoxygenation was monitored by ^{13}C NMR spectroscopy in an attempt to probe the mechanism through which triglycerides are converted to hydrocarbons over LDH catalysts. In order to facilitate the observation of reaction intermediates, the experiment was run under relatively mild conditions corresponding to deoxygenation over Ni-Mg-Al LDH at 300 °C, samples being taken for analysis after 1 h and 2 h. Additionally, a sample was analyzed after 4 h of reaction at 350 °C. Figure 27 shows the carbonyl region of the collected spectra, including that of the soybean oil starting material. As expected, the starting material showed signals at 172.5 and 172.1 ppm in a 2:1 ratio, which is characteristic of the ester carbonyl carbons of a triglyceride. After 1 h of reaction, these peaks became less intense and a new peak at 180.2 ppm arose, signaling both the consumption of the triglyceride and the formation of fatty acids whose carboxylic carbon accounts for the appearance of the new signal. After 2 h, the original peaks assigned to esters had completely disappeared, although the signal attributed to the carboxylic acids remained. Finally, after 4 h at 350 °C, no peaks were observed in the carboxylic region of the spectrum.

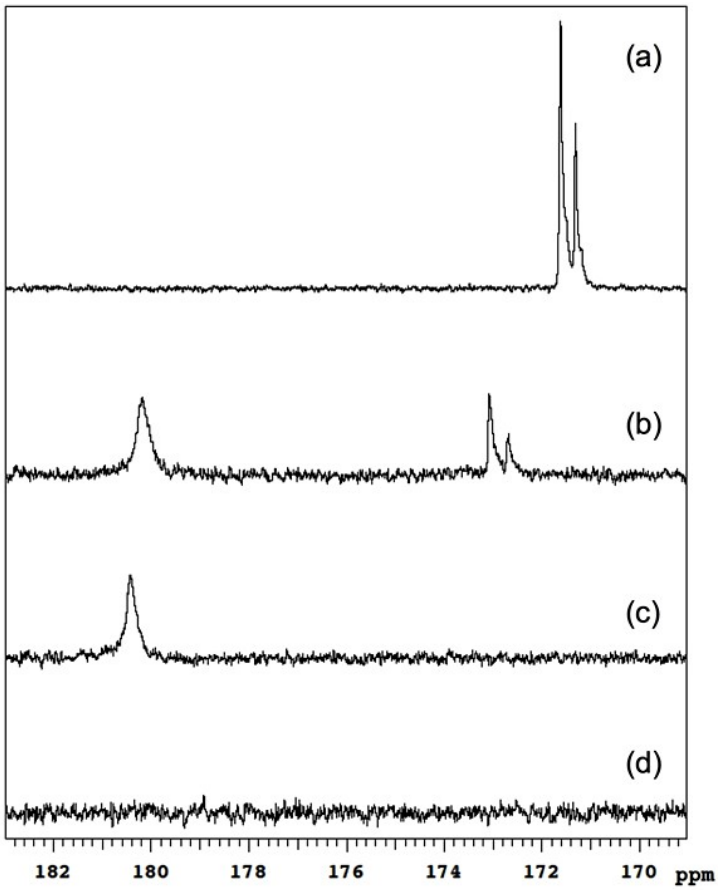

Figure 27. ^{13}C NMR spectra of liquid products obtained from soybean oil deoxygenation over Ni-Mg-Al: (a) initial soybean oil; (b) 300 °C, 1 h; (c) 300 °C, 2 h; (d) 350 °C, 4 h.

These observations are consistent with findings previously reported by us concerning the deoxygenation of soybean oil over 20 wt.% Ni/C . The formation of fatty acids from triglycerides is suggested to occur via a series of β-elimination reactions. A first β-elimination would yield a fatty acid molecule and an unsaturated diester. Notably, even in the absence of H_2, further elimination of another fatty acid equivalent from the unsaturated diester appears possible. In turn, the resulting fatty acids play the role of intermediates the decarboxylation/decarbonylation of which yields fuel-like hydrocarbons. Furthermore, during triglyceride deoxygenation, some degree of cracking of the fatty acid chains is observed, thereby providing additional pathways for hydrocarbon formation. The aforementioned process can is schematically shown in Figure 28.

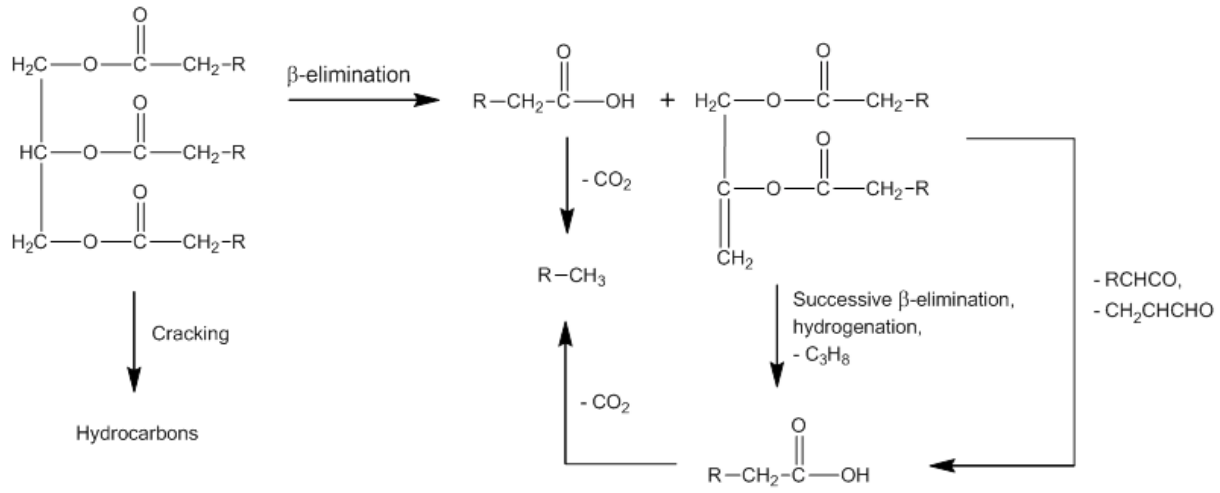

Figure 28. Suggested pathways for hydrocarbon formation during triglyceride deoxygenation.

The results of this study were both published in the Chemical Engineering Journal and included in a review article published in the Journal of Chemical Technology and Biotechnology . Moreover, these results were included in an abstract which was accepted and presented in the 22nd North American Catalysis Society Meeting in Detroit, Michigan [45].

Studies in a semi-batch reactor using carbon-supported Ni catalysts

Since it has been observed that the execution of deCOx reactions in semibatch mode – as opposed to batch mode – leads to better results by removing the evolved gases that would otherwise disfavor the reaction proceeding to completion and/or poison the metal surface (as would be the case with CO), fundamental studies on the decarboxylation of fatty acids and their derivatives over Ni catalysts were rounded off using a 100 mL semi-batch reactor. Four stearic acid deoxygenation experiments lasting 0, 0.5, 1 and 1.5 hours at 300 °C and 135 psi of pure H_2 were performed over a 20 wt.% Ni/C catalyst (the experiment lasting 0 hours corresponded to a run that was stopped immediately after the system had reached 300 °C to account for any reactions occurring during the heating period). Figure 29 summarizes the results of these experiments.

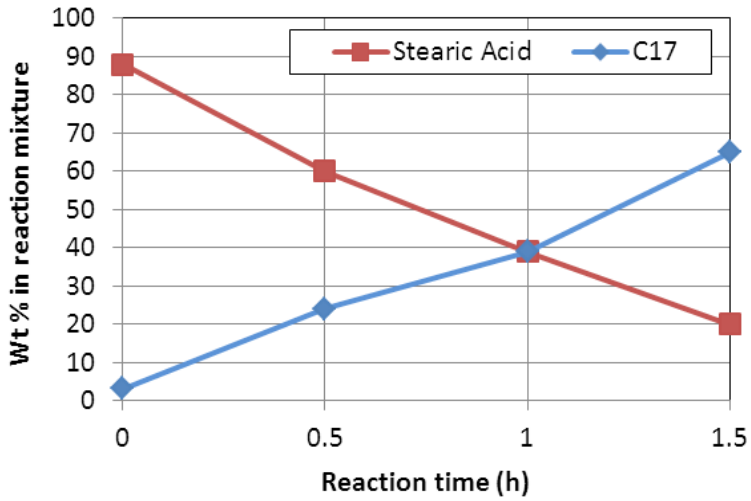

Figure 29. Feed consumption and product formation as a function of time during stearic acid deoxygenation over 20 wt.% Ni/C at 300 °C and 135 psi of pure H_2.

As Figure 29 clearly shows, heptadecane (C17) is produced as stearic acid is consumed throughout the experiment. Interestingly, the shape of these curves is consistent with a model in which stearic acid is converted to heptadecane *via* a decarboxylation reaction catalyzed by the carbon-supported metal catalyst.

Similarly, four tristearin deoxygenation experiments lasting 0, 2, 4 and 6 hours at 360 °C and 580 psi of pure H_2 were performed over 20 wt.% Ni/C. The results of these experiments are summarized in Figure 30.

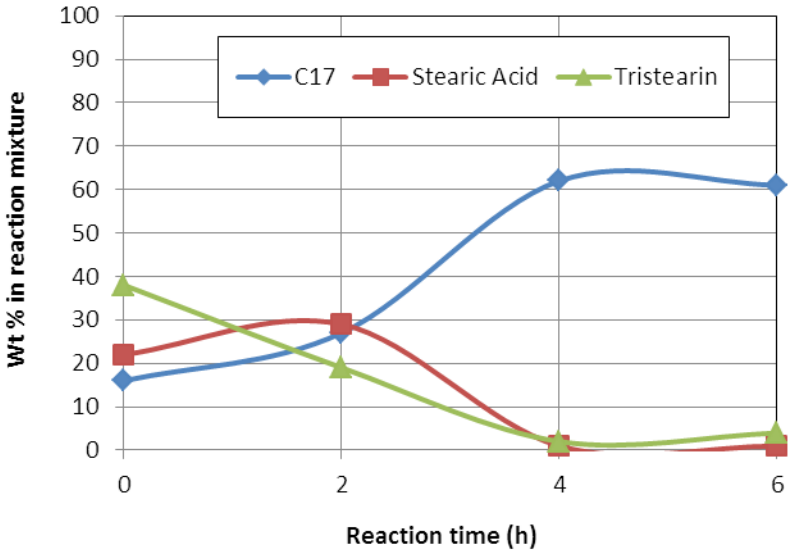

Figure 30. Feed consumption and product formation as a function of time during stearic acid deoxygenation over 20 wt.% Ni/C at 360 °C and 580 psi of pure H_2.

Notably, at t=0, the concentration of tristearin in the reaction mixture is ~38%. This suggests that a considerable amount of tristearin is converted during the time the system takes to reach the reaction temperature. The latter is in agreement with the presence of significant amounts of stearic acid and heptadecane at t=0, as these are the compounds produced when tristearin

reacts over Ni/C. Interestingly, the shape of the curves shown in Figure 30 also evinces the reaction path leading to the production of stearic acid and heptadecane: tristearin is first converted into stearic acid, which is then decarboxylated/decarbonylated to yield heptadecane, which is in agreement with the results of ^{13}C measurements included in our Topics in Catalysis and Chemical Engineering Journal publications.

Improvements in the GC method used to analyze the products of this reaction – the deoxygenation *via* decarboxylation of tristearin and stearic acid – have allowed for a better comparison to be made between the performance of different catalysts in terms of their ability to convert triglycerides and fatty acids into fuel-like hydrocarbons. This is illustrated by the boiling point distribution plots shown in Figure 31.

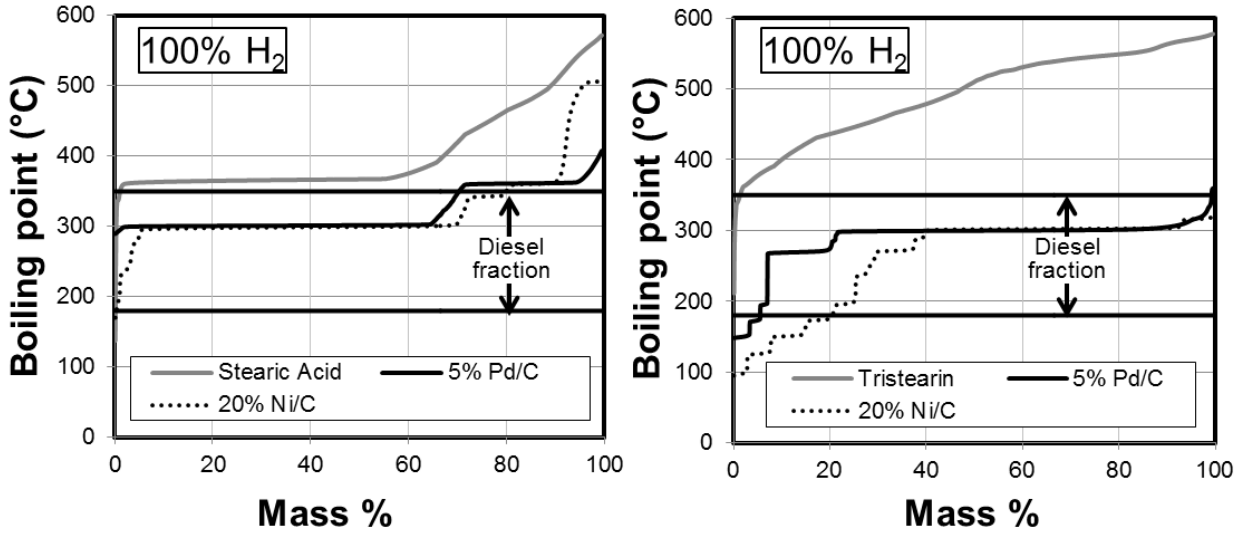

Figure 31. Boiling point distribution plots from simulated distillation GC analysis of products obtained from the deoxygenation of stearic acid (left) and tristearin (right) over 20%Ni/C and 5% Pd/C under a H_2 atmosphere in semi-batch mode.

These plots reveal that most of the components in the various product mixtures boil within the diesel fuel range (180-350 °C), regardless of the nature of the feedstock and the catalyst employed. Nevertheless, both the specific amount and the boiling point distribution of the reaction products *within the diesel fraction* show a clear dependence on both the feed and the catalyst used. In general, while Pd/C favors the formation of C17, Ni-based catalysts also tend to produce lighter products in the C10-C17 range (which may be advantageous for fuel blending purposes). From the plots included in Figure 31, it is clear that inexpensive Ni-based catalysts can afford comparable amounts of fuel-like hydrocarbons as those obtained using Pd/C. These – and similar plots acquired for the products obtained for experiments run under 10% H_2/N_2 – were included in an article published in the journal Fuel and in two abstracts which were accepted and presented in the 7th International Conference in Environmental Catalysis (ICEC) in Lyon, France [46] and in the 2012 Annual Meeting of the American Institute of Chemical Engineers [47].

Studies in a semi-batch reactor using carbon-supported Ni catalysts promoted with Cu or Sn
It has been shown that inexpensive Ni-based catalysts can afford comparable amounts of fuel-like hydrocarbons *via* deCO_x as those obtained using Pd/C, the costly catalyst commonly used to catalyze this reaction. However, previous literature reports suggest that further

improvements could also be made by fine-tuning the activity of the catalytically active phase through the promotion of Ni with Cu or Sn. With this in mind, carbon-supported Ni-Cu and Ni-Sn catalysts have been prepared and tested in the conversion of triglycerides and fatty acids to hydrocarbons (see Table 9).

Table 9. Decarboxylation of tristearin (360 °C, 580 psi, 6 h) and stearic acid (300 °C, 135 psi, 1.5 h) over carbon-supported Ni, Ni-Cu and Ni-Sn catalysts*.

Catalyst	Feed	Gas	Conversion (%)	Selectivity to C10-C17 (%)	Selectivity to C17 (%)
20% Ni/C	Tristearin	H_2	98	90	68
20% Ni - 1% Cu/C	Tristearin	H_2	78	96	64
20% Ni – 1% Sn/C	Tristearin	H_2	79	97	60
20% Ni/C	Stearic acid	H_2	71	>99	10
20% Ni – 1% Sn/C	Stearic acid	H_2	38	>99	31

*Semi-batch reactor, 0.5 g catalyst, 1.8 g substrate, dodecane (25 ml) as solvent. Catalyst reduced *in situ* at 350 ºC under flowing 10% H_2/N_2 for 3 h prior to experiment.

These preliminary results clearly illustrate that the selectivity to C10-C17 hydrocarbons shown by a carbon-supported Ni catalyst can indeed be improved upon addition of Cu or Sn when tristearin is used as the feed. Likewise, these results make patent that with respect to the Ni-only catalyst, Ni-Sn displays higher selectivity to C17 when stearic acid is employed. These results are promising, particularly taking into account that the generation of these data involved no optimization work whatsoever. In fact, given the number of variables that could be systematically altered in an effort to improve on these results (total metal loading, Ni/Cu or Ni/Sn ratio, metal particle size, catalyst preparation method, catalyst pretreatment, etc.), considerably better results are expected once optimization efforts are undertaken.

Admittedly, the addition of Cu or Sn was accompanied by a drop in conversion. This was to be expected, as both Cu and Sn are less intrinsically active than Ni in decarboxylation. However, from an industrial standpoint, improvements in selectivity have inherent advantages that almost invariably offset any concomitant loss in activity. In our case, the Ni-Cu and Ni-Sn catalysts tested managed to maintain most of the conversion shown by Ni-only catalysts while also delivering noticeable improvements in the selectivity towards the desired products. Therefore, these formulations can be considered promising catalysts for the conversion of lipids to hydrocarbons. Fundamental studies are necessary to rationalize – and thereby capitalize on – these results. To this end, a research proposal has been prepared for submission to the National Science Foundation's Division of Chemistry. In short, the proposed work has as its main objectives: 1) to understand the mechanism through which the electronic or morphological fine-tuning of the active phase within Ni-based $deCO_x$ catalysts can lead to improvements in selectivity and/or durability; and 2) to elucidate the reaction mechanism of lipid $deCO_x$ over Ni-based catalysts through the identification of reaction intermediates under realistic operating conditions.

Studies in a semi-batch reactor using Ni-based catalysts comprising oxidic supports

Efforts were made to identify affordable Ni-based $deCO_x$ catalysts that would be amenable to reactivation by treatment in hot air – the regeneration method favored by industry due to its low cost and simplicity – while also offering the possibility to study catalyst coking *via* TGA. To this end, supported Ni catalysts that do not comprise carbon as the support were prepared and tested for activity in the deoxygenation of tristearin (a model triglyceride) *via* $deCO_x$ under a pure

hydrogen atmosphere. Ceria and zirconia were chosen based on previous reports touting these oxides as the most promising supports for catalytic deoxygenation applications and alumina was chosen as a reference oxide [48]. Additionally, the use of a Layered Double Hydroxide (LDH) catalyst containing both Ni and Al (henceforth referred to as Ni-Al LDH) was also investigated. Finally, the oxide-supported Ni catalysts showing the most promising performance under pure hydrogen were tested under 10% H_2/N_2 and under pure nitrogen. Table 10 shows the results of these catalytic activity tests.

Table 10. Tristearin deCO_x over oxide-supported Ni catalysts at 360 °C and 580 psi.

Catalyst	Feed	Gas	Conversion (%)	Selectivity to C10-C17 (%)*	Selectivity to C17 (%)*
20% Ni/CeO_2	Tristearin	H_2	98	62 (61)	4 (4)
20% Ni/ZrO_2	Tristearin	H_2	>99	45 (45)	<1 (<1)
20% Ni/Al_2O_3	Tristearin	H_2	96	71 (68)	36 (35)
20% Ni/Al_2O_3	Tristearin	10% H_2/N_2	>99	57 (56)	2 (2)
20% Ni/Al_2O_3	Tristearin	N_2	86	58 (50)	31 (27)
Ni-Al LDH	Tristearin	H_2	81	86 (70)	69 (56)
Ni-Al LDH	Tristearin	10% H_2/N_2	90	72 (65)	40 (36)
Ni-Al LDH	Tristearin	N_2	88	70 (62)	40 (35)

* Numbers in parentheses represent corresponding yield (conversion × selectivity) values

Interestingly, although the alumina-supported Ni catalyst afforded the best yields of diesel-like (decane-heptadecane or C10-C17) hydrocarbons amongst the catalysts supported on simple oxides, the best results were obtained over the Ni-Al LDH catalyst. Indeed, when Ni-AL LDH was tested in the deCO_x of tristearin under a hydrogen atmosphere, this catalyst proved capable of achieving C10-C17 and C17 yields of 70 and 56%, respectively (for comparison purposes, a 20% Ni/carbon catalysts displays C10-C17 and C17 yields of 76 and 54% under the same conditions). This clearly indicates that Ni-based catalysts with supports other than carbon can afford comparable results to those obtained over carbon-supported Ni. Additionally, the fact that these materials can be submitted to TGA in air without the interference of the support, allowed us to study the effect of H_2 partial pressure and catalyst acidity on deCO_x performance. To this end, the TGA in air of the spent catalysts was performed in order to determine the extent of coking (see Figure 32) and the ammonia temperature programmed desorption (NH_3-TPD) of both Ni-Al LDH and 20 wt.% Ni/Al_2O_3 was acquired to gauge the acidity of these formulations (see Figure 33).

Interestingly, the trends followed by the TGA plots in Figure 32 and the C10-C17 yields in Table 10 show a remarkable correspondence. Indeed, the amount of carbonaceous deposits on the spent catalysts decreased monotonically with increasing H_2 partial pressure and consistently lower amounts of deposits were obtained over Ni-Al LDH than over 20 wt% Ni/Al_2O_3 regardless of the reaction atmosphere. This clearly illustrates the interplay between H_2 partial pressure and acidity: whereas H_2 manages to curb the formation of coke deposits *via* the hydrogenation of unsaturated species, acidity – particularly weak and medium strength acid sites according to the results of NH_3-TPD (Figure 33) – appears to favor the formation of these deposits.

In order to test the recyclability of these formulations, the Ni-Al LDH catalyst spent under 10% H_2/N_2 – which according to TGA contained 20 wt.% of carbonaceous deposits (see Figure 32) – was calcined under air at 500 °C for 6 h prior to being retested. As Tables 11 and 12 show, both the textural properties (surface area and porosity) and the catalytic performance of a spent Ni-Al LDH catalyst can be reestablished – i.e., the catalyst can be regenerated and recycled – by treatment in hot air, which makes this formulation particularly interesting from an industrial stand point.

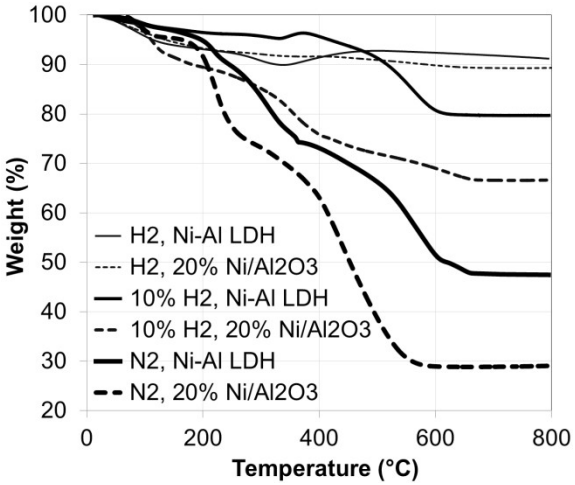

Figure 32. TGA plots of Ni catalysts spent in tristearin deCO$_x$ under different atmospheres

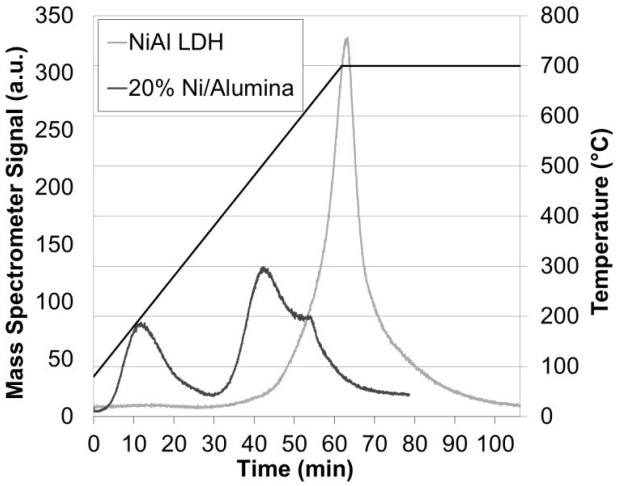

Figure 33. NH_3-TPD profiles showing the different acidity of Ni-Al LDH and 20 wt.% Ni/Al_2O_3

Table 11. Textural properties of Ni-Al LDH catalysts[†].

Catalyst	BET surface area (m^2/g)	Pore volume (cm^3/g)	Avg. Pore diameter (nm)
Fresh Ni-Al LDH	162	0.33	7.1
Spent Ni-Al LDH	97	0.32	6.7
Regenerated Ni-Al LDH	147	0.60	8.2

[†]Spent in a tristearin reaction performed under 10% H_2/N_2. Regeneration comprised calcination removed >95% of the carbon deposits according to TGA.

Table 12. Deoxygenation of tristearin *via* deCO$_x$ under 10% H_2/N_2 over Ni-Al LDH catalyst[‡].

Catalyst	Conversion (%)	Selectivity to C10-C17 (%)*	Selectivity to C17 (%)*
Fresh Ni-Al LDH	90	72 (65)	40 (36)
Spent Ni-Al LDH	68	71 (48)	47 (32)
Regenerated Ni-Al LDH	93	81 (75)	45 (42)

[‡]0.59 g of spent catalyst used to account for the weight of carbonaceous deposits. Regeneration removed >95% of the carbon deposits according to TGA.

These results have been included in a manuscript recently submitted for publication to the journal Energy & Fuels [49].

In summary, work performed in our laboratory has shown that good yields of fuel-like hydrocarbons can be obtained from the fatty acids and the triglycerides that constitute vegetable and algae oils *via* $deCO_x$. This approach show several advantages over hydrotreating, which is the method currently employed to achieve this transformation. Indeed, whereas hydrotreating necessitates high pressures of hydrogen and problematic sulfided catalysts, $deCO_x$ can proceed under considerably low hydrogen pressures and over simple metal catalysts. Although initial reports on this alternative deoxygenation approach focused on the use of catalysts comprising costly Pd or Pt, our work has shown that inexpensive Ni-based catalysts can offer comparable $deCO_x$ performance than formulations based on these precious metals. Advances have also been made with regards to the materials used as catalyst supports, as reports by other workers had focused on the use of activated carbon as the carrier in $deCO_x$ catalysts. Given that these catalysts are susceptible to deactivation by the accumulation of carbonaceous deposits on their surface and the use of a carbon support both complicates the study of spent catalysts *via* thermogravimetric analysis (TGA) and precludes the regeneration of the catalyst through the combustion of these deposits, efforts were made to develop non-precious metal catalysts comprising oxidic supports. Notably, our work has shown that oxide-supported Ni on oxide supports and hydrotalcite materials have the ability to rival – and in some cases outperform – carbon-supported Pd, Pt, or Ni. The analysis of the spent catalysts comprising Ni on oxidic supports has allowed us to show that catalytic performance is determined by the interplay between hydrogen partial pressure and catalyst acidity, an effect which has been observed to be feed-dependent and explainable in terms of catalyst fouling. Finally, recycling studies have shown that the entirety of the activity and selectivity of Ni-based catalysts can be regained treatment in hot air – the catalyst regeneration approach favored by industry due to its low cost and simplicity.

3. Conclusions

The University of Kentucky Biofuels Laboratory is now complete and fully functional. In keeping with the open laboratory objective, experiments and sample analyses have been performed in the Laboratory at the request of other institutions (both within and outside Kentucky), as well as other research groups at the University of Kentucky. Initial research at the laboratory has focused on three main technical areas: (i) the identification of algae strains suitable for oil production, utilizing flue gas from coal-fired power plants as a source of CO_2; (ii) the conversion of algae to biofuels; and (iii) the development of methods for the analysis of lignin and its deconstruction products. Although the Department of Energy grant which funded the creation of this laboratory has now expired, work is continuing in all three of these areas, through a mix of federal, state, industrial and internal grants. Indeed, the infrastructure provided by the DOE grant has proved to be critical for the acquisition of new funding.

Specific highlights of the research performed to date include:

- Identification of the optimal pH, growth media and water source for *Scenedesmus* sp. cultivation, in order to support a University of Kentucky project aimed at recycling CO_2 emissions using algae. Additionally, a screening study was completed in order to identify promising strains for use under winter conditions. Of the 60 candidate strains identified from the literature, *Haematococcus droebakensis, Bracteacoccus minor, Neochloris wimmeri, Chlorella luteoviridis, Chlorella sorokiniana, Chlorella regularis, Chlorella kessleri,*

Stichococcus bacillaris, Chlorella vulgaris, and *Tetraspora sp.* were found to afford the highest growth rates under the conditions used.

- Fast pyrolysis of *Scenedesmus* algae was conducted at two reactor scales in order to compare and understand the origin of the products formed. Product analysis showed the various fractions of bio-oil produced were, in certain respects, comparable to pyrolysis products from wood and other microalgae species. Indeed, the oxygen and moisture contents of the products were typical of pyrolysis oil produced from lignocellulosic feedstock. However, the products possessed a relatively high nitrogen content due to the high protein content in the algae feedstock.

- The development of a method for the reliable determination of sinapyl:guaiacyl (S:G) monomer ratios in lignin based on pyrolysis-GC/MS. Having obtained the pyrolysis profile of physical mixtures of sinapyl and coniferyl alcohols (mixed in different mole ratios), marker pyrolysates for the calculation of the S:G ratio in lignin can be carefully selected according to unique samples. These marker groups can then be calibrated against known S:G ratios to provide analysis of the actual S:G ratio of lignin in biomass.

- The identification of a class of Ni catalysts which are active catalysts for the deoxygenation of fatty acids and triglycerides – to afford hydrocarbons in the diesel fuel range - via decarboxylation and decarbonylation. This approach shows several advantages over hydrotreating; indeed, whereas hydrotreating necessitates high pressures of hydrogen and problematic sulfided catalysts, deCO_x can proceed under considerably low hydrogen pressures and over simple metal catalysts. Insights have also been gained with respect to the mechanism of triglyceride deoxygenation.

4. Publications and Presentations

Publications - since project inception:

1. A.E. Harman-Ware, M. Crocker, A. Preet Kaur, M.S. Meier, D. Kato, B. Lynn, Pyrolysis-GC/MS of sinapyl and coniferyl alcohol, *J. Anal. Appl. Pyrol*., 99 (2013) 161.
2. E. Santillan-Jimenez, T. Morgan, J. Lacny, S. Mohapatra, M. Crocker, Catalytic deoxygenation of triglycerides and fatty acids over carbon-supported nickel, *Fuel* 103 (2013) 1010.
3. E. Santillan-Jimenez, M. Crocker, Catalytic deoxygenation of fatty acids and their derivatives to hydrocarbon fuels via decarboxylation/decarbonylation, *J. Chem. Technol. Biotechnol*., 87 (2012) 1041.
4. T. Morgan, E. Santillan-Jimenez, A.E. Harman-Ware, Y. Ji, D. Grubb, M. Crocker, Catalytic deoxygenation of triglycerides to hydrocarbons over supported nickel catalysts, *Chem. Eng. J*., 189-190 (2012) 346.
5. V. Mendu, A.E. Harman-Ware, M. Crocker, J. Jae, J. Stork, S. Morton III, A. Placido, G. Huber, S. DeBolt, Identification and thermochemical analysis of high-lignin feedstocks for biofuel and biochemical production, *Biotechnol. Biofuels*, 4 (2011) 43.
6. T. Morgan, D. Grubb, E. Santillan-Jimenez, M. Crocker, Conversion of Triglycerides to Hydrocarbons over Supported Metal Catalysts, *Top. Catal*., 53 (2010) 820.

Publications – submitted and in preparation:

1. C. Crofcheck, A. Shea, M. Montross, M. Crocker, R. Andrews, Influence of flue gas components on the growth rate of *Chlorella vulgaris* and *Scenedesmus acutus* utilized for CO_2 mitigation, J. Biochem. Technol., submitted September 2012.
2. C. Crofcheck, X. E, *A. Shea*, M. Montross, M. Crocker, R. Andrews, Influence of media composition on the growth rate of *Chlorella vulgaris* and *Scenedesmus acutus* utilized for CO_2 mitigation, Transactions of the ASABE, submitted December 2012.
3. A.E. Harman-Ware, T. Morgan, M. Wilson, M. Crocker, J. Zhang, K. Liu, J. Stork, S. Debolt, Microalgae as a renewable fuel source: fast pyrolysis of *Scenedesmus* sp., Renewable Energy, submitted December 2012.
4, E. Santillan-Jimenez, T. Morgan, J. Shoup, M. Crocker, “Catalytic deoxygenation of triglycerides and fatty acids to hydrocarbons over Ni-Al layered double hydroxide”, to be submitted to Energy & Fuels.
4. C. Petti, A.E. Harman-Ware, A. Shearer, M. Tateno, A.B. Downie, M. Crocker, S. DeBolt, Phenylpropanoid sorghum mutant displays antithetic leaf shoot saccharification properties, journal to be decided.
5. X. E, C. Crofcheck, J. Aurandt, Nutrients recycling strategies for microalgae-based CO_2 bio-mitigation system, journal to be decided.
6. X. E, C. Crofcheck, J. Aurandt, Anaerobic Digestion of *Scenedemus* with Thermal-chemical Pretreatment, journal to be decided.
7. X. E, C. Crofcheck, M. Montross, Life cycle assessment (LCA) of the microalgae-based CO_2 mitigation system, journal to be decided.

Conference presentations:

1. A.E. Harman-Ware, M. Crocker, S. DeBolt, Pyrolysis-GC/MS characterization of biomass, poster presentation at the 2013 Kentucky Statewide Workshop: Renewable Energy & Energy Efficiency, Louisville, KY, March 24-26.
2. M. Crocker, J. Mobley, A.E. Harman-Ware, R. Pace, S. Morton III, N. Patil, M. Meier, S. DeBolt, Lignin Deconstruction for the Production of Fuels and Chemicals, oral presentation at the 1st SEC Symposium, Impact of the Southeast on the World’s Renewable Energy Future, Atlanta, GA, February 10-12, 2013.
3. T. Graham, C. Crofcheck, A. Shea, M. Montross, M. Crocker, R. Andrews, Investigation of Media Ingredients and Water Sources for Algae CO_2 Capture at Different Scales to Demonstrate the Correlations Between Lab-scale and Large-Scale Growth, poster presentation at the 1st SEC Symposium, Impact of the Southeast on the World’s Renewable Energy Future, Atlanta, GA, February 10-12, 2013.
4. L. Mills, A.E. Harman-Ware, J. Groppo, R. Pace, A. Placido, M. Wilson, S.A. Morton III, M. Crocker, Microalgae Cultivation in Closed-Loop Photobioreactors: Biofilm Characterization, Prevention and Removal, Annual Meeting of the American Institute of Chemical Engineers (student conference), Pittsburg, PA, October 26-29, 2012.

5. J. Shoup, E. Santillan-Jimenez, T. Morgan, M. Crocker, Conversion of Triglycerides and Fatty Acids to Hydrocarbons Using Supported Nickel Catalysts, Annual Meeting of the American Institute of Chemical Engineers (student conference), Pittsburg, PA, October 26-29, 2012.
6. E. Santillan-Jimenez, T. Morgan, M. Crocker, Conversion of triglycerides and fatty acids to hydrocarbons via decarboxylation/decarbonylation ($deCO_x$) over supported nickel catalysts, poster presentation at the 7th International Conference on Environmental Catalysis, Lyon, France, September 2-6, 2012.
7. A.E. Harman-Ware, M. Crocker, S. DeBolt, Pyrolysis-GC/MS characterization of biomass, oral presentation at the 244th ACS National Meeting, Philadelphia, August 19-23, 2012, IEC-25.
8. R. Andrews, M. Crocker, S. DeBolt, M. Meier, S.A. Morton, Lignin deconstruction for the production of liquid fuels and chemicals, oral presentation at the 244th ACS National Meeting, Philadelphia, August 19-23, 2012, IEC-24.
9. S.A. Morton III, R. Andrews, M. Crocker, C. Crofcheck, J. Groppo, A. Placido, Mitigation of CO_2 from a coal-fired power plant using microalgae: Development and demonstration, poster presentation at the 2nd International Conference on Algal Biomass, Biofuels and Bioproducts, San Diego, June 10-13, 2012.
10. C. Crofcheck, X. E, A. Shea, M. Montross, M. Crocker, R. Andrews, Influence of media composition and flue gas components on the growth rate of *Chlorella vulgaris* and *Scenedesmus* to be utilized for CO_2 mitigation, Podium presentation at the Annual Institute of Biological Engineering Meeting, Indianapolis, IN, March 2012.
11. A. Hickman, T. Mains, M. Ritchie, C. Zheng, C. Crofcheck, A. Shea, Real-Time Algae Growth System: A Senior Design Project, Poster presented at the Annual Institute of Biological Engineering Meeting, Indianapolis, IN, March 2012.
12. X. E, A. Shea, C. Crofcheck, M. Montross, M. Crocker, R. Andrews, J. Aurandt, O. Hayden, Incorporation of nutrient recycling and anaerobic digestion in a CO_2 mitigation algae cultivation system, Poster presented at the Annual Institute of Biological Engineering Meeting, Indianapolis, IN, March 2012.
13. L. Ware, T. Morgan, M. Wilson, S. Mohapatra, M. Crocker, J. Zhang, K. Liu, Fast pyrolysis of *Scenedesmus* algae, poster presentation at the 242nd ACS National Meeting, Denver, CO, August 28-September 1, 2011, FUEL-152; Preprints of Symposia - American Chemical Society, Division of Fuel Chemistry, 2011, 56(2), 533-534.
14. C. Crofcheck, A. Shea, M. Montross, R. Andrews, M. Crocker, Medium and Growth Optimization for *Scenedesmus* for CO_2 Mitigation of Flue Gas, ASABE Annual International Meeting in Louisville, KY, August 2011.
15. K. Cassidy, C. Crofcheck, M. Montross, A. Shea,. Evaluating Algal Growth in Different Temperatures, ASABE Annual International Meeting in Louisville, KY, August 2011.
16. S. Mohapatra, T. Morgan, E. Santillan-Jimenez, M. Crocker, Conversion of Triglycerides and Fatty Acids to Hydrocarbons over Supported Nickel Catalysts, poster presentation (P-Tu-53) at the 22nd North American Catalysis Society Meeting, June 5-10, 2011, Detroit, MI.
17. J. Mobley, L. Ware, E. Santillan-Jimenez, A. Placido, R. Andrews, M. Crocker, S. DeBolt, M. Meier, S.A. Morton III, Dissolution and Analysis of Lignin-Rich Biomass Feedstocks,

2011 Kentucky Renewable Energy & Energy Efficiency Workshop, Louisville, KY, March 14, 2011.

18. K. Cassidy, C. Crofcheck, M. Montross, A. Shea, R. Andrews, M. Crocker, S. Morton, C. Fisk, Evaluating Algal Growth in Different Temperatures, Annual Institute of Biological Engineering Meeting, Atlanta, GA, March, 2011.
19. T. Graham, N. Rhea, A. Shea, C. Crofcheck, M. Montross, Evaluation of PBR Material of Construction on the Growth of Algae, Annual Institute of Biological Engineering Meeting, Atlanta, GA, March, 2011.
20. C. Crofcheck, S. Short, M. Montross, A. Shea, W. Chen, W. Adams, R. Andrews, M. Crocker, S. Morton, Optimization of Algal Medium for CO2 Mitigation from Flue Gas, ASABE Annual International Meeting in Pittsburg, PA, June, 2010.
21. Cassidy, K., C. Crofcheck, M. Montross, A.Shea, W. Chen, W. Adams, R. Andrews, M. Crocker, S. Morton, C. Fisk, Algal Response to Variations in Temperature. ASABE Annual International Meeting in Pittsburg, PA, June, 2010.
22. C. Fisk, M. Wilson, A. Placido, S. Morton, R. Andrews, M. Crocker, J. Groppo, C. Crofcheck, M. Montross, Development of an Algae-Based System for CO_2 Mitigation from Coal-Fired Power Plants, ASABE Annual International Meeting in Pittsburg, PA, June, 2010.
23. K. Cassidy, C. Crofcheck, M. Montross, A.Shea, W. Chen, W. Adams, R. Andrews, M. Crocker, S. Morton, C. Fisk, Algal Response to Variations in Temperature. Annual Institute of Biological Engineering Meeting in Cambridge, MA, March, 2010.
24. C. Crofcheck, M. Montross, K. Cassidy, A. Kroumov, A. Shea, W. Chen, R. Andrews, M. Crocker, S. Morton, C. Fisk, M. Wilson, Medium Optimization for CO_2 Mitigation from Flue Gas, Annual Institute of Biological Engineering Meeting in Cambridge, MA, March, 2010.

5. References

[1] D. Harris, S. Debolt, Synthesis, regulation and utilization of lignocellulosic biomass, *Plant Biotechnol. J.* 8 (2010) 244.

[2] V.H. Dale, K.L. Kline, J. Wiens, J. Fargione, Biofuels: implications for land use and biodiversity, *Washington, DC: Ecological Society of America,* 2010: http://www.esa.org/biofuelsreports/files/ESA%20Biofuels%20Report_VH%20Dale%20et%20al.pdf.

[3] T.P. Vispute, H. Zhang, A. Sanna, R. Xiao, G.W. Huber, Renewable Chemical Commodity Feedstocks from Integrated Catalytic Processing of Pyrolysis Oils, *Science* 330 (2010) 1222.

[4] J.H. Jae, G.A. Tompsett, Y.C. Lin *et al.,* Depolymerization of lignocellulosic biomass to fuel precursors: maximizing carbon efficiency by combining hydrolysis with pyrolysis, *Energy & Environmental Sci.* 3 (2010) 358.

[5] J. Zakzeski, P. Bruijnincx, A. Jongerius, B. Weckhuysen, The Catalytic Valorization of Lignin for the Production of Renewable Chemicals, *Chem. Rev.* 110 (2010) 3552.

[6] V. Mendu, A.E. Harman-Ware, M. Crocker, J. Jae, J. Stork, S.A. Morton, A. Placido, Identification and thermochemical analysis of high-lignin feedstocks for biofuel and biochemical production, *Biotechnol. Biofuels* 4 (2011) 43.

[7] A.E. Harman-Ware, M. Crocker, A.P. Kaur, M.S. Meier, D. Kato, B. Lynn, Pyrolysis-GC/MS of Sinapyl and Coniferyl Alcohol, *J. Anal. Appl. Pyrol.* 99 (2012) 161-169.

[8] C. Saiz-Jimenez, J.F. De Leeuw, Lignin Pyrolysis Products: Their Structures and Their Significance as Biomarkers, *Advances in Organic Geochemistry* 10 (1985) 869-876.

[9] P.R. Patwardhan, D.L. Dalluge, B.H. Shanks, R.C. Brown, Distinguishing primary and secondary reactions of cellulose pyrolysis, *Bioresource Technol.* 102(8) (2011) 5265-5269.

[10] J.J. Boon, Amino Acid Sequence Information in Proteins and Complex Proteinaceous Material Revealed by Pyrolysis-Capillary Gas Chromatograph-Low and High Resolution Mass Spectrometry, J. Anal. Appl. Pyrol. 11 (1987) 313-327.

[11] A.V. Gidh et al., *Determination of lignin by size exclusion chromatography using multi angle laser light scattering.* Journal of Chromatography A, 2006. **1114**(1): p. 102-110.

[12] A.F.M. Barton, *CRC Handbook of Solubility Parameters and other Cohesion Parameters*1983, Boca Raton, Fl.: CRC. 594.

[13] A.E. Harman-Ware, T. Morgan, M. Wilson, M. Crocker, J. Zhang, K. Liu, J. Stork, S. Debolt, Microalgae as a renewable fuel source: fast pyrolysis of *Scenedesmus* sp., Renewable Energy, submitted.

[14] D. Badaut, F. Risacher, Authigenic smectite on diatom frustules in Bolivian saline lakes, Geochimica et Cosmochimica Acta 47 (1983) 363-375.

[15] D. Mohan, C.U. Pittman, P.H. Steele, Pyrolysis of Wood/Biomass for Bio-oil: A Critical Review. Energy Fuels 20 (2006) 848-889.

[16] X. Miao, Q. Wu, High yield bio-oil production from fast pyrolysis by metabolic controlling of Chlorella protothecoides, J. Biotechnol. 110 (2004) 85-93.

[17] X. Miao, Q. Wu, C. Yang, Fast *pyrolysis* of microalgae to produce renewable fuel, J. Anal. Appl. Pyrol. 71 (2004) 855-63.

[18] I.V. Babich, M. van der Hulst, L. Lefferts, J.A. Moulijn, P. O'Connor, K. Seshan, Catalytic pyrolysis of microalgae to high-quality liquid bio-fuels, Biomass Bioenergy 35 (2011) 3199-3207.

[18] G. P. Shulman, P.G. Simmonds, Thermal decomposition of aromatic and heteroaromatic amino-acids, Chem. Comm. London (1968) 1040-1042.

[19] G. Chiavari, G.C. Galletti, Pyrolysis—gas chromatography/mass spectrometry of amino acids, J. Anal. Appl. Pyrol. 24 (1991) 123-137.

[20] M.A. Ratcliff, E.E. Medley, P.G. Simmonds, Pyrolysis of amino acids. Mechanistic considerations, J. Org. Chem. 39 (1974) 1481-1490.

[21] T.M. Brown, P. Duan, P.E. Savage, Hydrothermal liquefaction and gasification of Nanochloropsis sp., Energy Fuels 24 (2010) 3639-46.

[22] S. Tsuge, H. Matsubara, High Resolution Pyrolysis-Gas Chromatography of Proteins and Related Materials, J. Anal. Appl. Pyrol. 8 (1985) 49-64.

[23] J.W. Alencar, P.B. Alves, A.A. Craveiro, Pyrolysis of tropical vegetable oils, J. Agric. Food Chem. 31 (1983) 1268-1270.

[24] C. Chang, S. Wan, China's motor fuels from tung oil, Ind. Eng. Chem. 39 (1947) 1543-1548.

[25] K. Kitamura, Studies of the Pyrolysis of Triglycerides, Bull. Chem. Soc. Japan 44 (1971) 1606-1609.

[26] W.W. Nawar, Thermal Degredation of Lipids, J. Agric. Food Chem. 17 (1969) 18-21.

[27] P. Nichols, R. Holman, Pyrolysis of saturated triglycerides, Lipids 7 (1972) 773-779.

[28] A.W. Schwab, G.J. Dykstra, E. Selke, S.C. Sorenson, E.H. Pryde, Diesel Fuel from Thermal Decomposition of Soybean oil, J. Amer. Oil Chem. Soc. 65 **(**1988) 1781-1786.

[29] R.O. Idem, S.P.R. Katikaneni, N.N. Bakhshi, Thermal Cracking of Canola Oil: Reaction Products in the Presence and Absence of Steam, Energy Fuels 10 (1996) 1150-1162.

[30] A. Campanella, R. Muncrief, M. P. Harold, D.C. Griffith, N.M. Whitton, R. S. Weber, Thermolysis of microalgae and duckweed in a CO_2-swept fixed-bed reactor: Bio-oil yield and compositional effects, Bioresource Technol. 109 (2012) 154-162.

[31] T. Mata, A. Martins, N. Caetano, Microalgae for Biodiesel Production and other Applications: A Review, Renew. Sustain. Energy Rev. 14 (2010) 217-232.

[32] B. Wang, Y. Li, N. Wu, C. Lan, CO_2 bio-mitigation using microalgae, Appl. Microbiol. Biotechnol. 79 (2008) 707-718.

[33] L. Brennan, P. Owende, Biofuels from microalgae—A review of technologies for production, processing, and extractions of biofuels and co-products, Renew. Sustain. Energy Rev. 14 (2010) 557-577.

[34] E.G. Bligh, W.J. Dyer, A rapid method of total lipid extraction and purification, Can. J. Biochem. Physiol. 37 (1959) 911-917.

[35] A. Hara, N Radin, Lipid extraction of tissues with a low-toxicity solvent. Anal. Biochem. 90 (1978) 420-426.

[36] T. Morgan, E. Santillan-Jimenez, A.E. Harman-Ware, Y. Ji, D. Grubb, M. Crocker, Catalytic deoxygenation of triglycerides to hydrocarbons over supported nickel catalysts, Chem. Eng. J. 189-190 (2012) 346-355.

[37] T. Morgan, D. Grubb, E. Santillan-Jimenez, M. Crocker, Conversion of triglycerides to hydrocarbons over supported metal catalysts, Top. Catal. 53 (2010) 820-829.

[38] E. Santillan-Jimenez, T. Morgan, J. Lacny, S. Mohapatra, M. Crocker, Catalytic deoxygenation of triglycerides and fatty acids to hydrocarbons over carbon-supported nickel, Fuel 103 (2013) 1010-1017.

[39] W.F. Maier, W. Roth, I. Thies, P.V.R. Schleyer, Hydrogenolysis IV. Gas phase decarboxylation of carboxylic acids, Chem. Ber. 115 (1982) 808-812.

[40] R. Stern, G. Hillion, Process for manufacturing a linear olefin from a saturated fatty acid or fatty acid ester, U.S. Patent Number 4554397 (1985).

[41] P. Mäki-Arvela, I. Kubickova, M. Snåre, K. Eränen, D.Y. Murzin, Catalytic deoxygenation of fatty acids and their derivatives, Energy Fuels 21 (2007) 30-41.

[42] M. Snåre, I. Kubicková, P. Mäki-Arvela, D. Chichova, K. Eränen, D.Y. Murzin, Catalytic deoxygenation of unsaturated renewable feedstocks for production of diesel fuel hydrocarbons, Fuel 87 (2008) 933-945.

[43] P.T. Do, M. Chiappero, L.L. Lobban, D.E. Resasco, Catalytic deoxygenation of methyl-octanoate and methyl-stearate on Pt/Al_2O_3, Catal. Lett. 130 (2009) 9-18.

[44] E. Santillan-Jimenez, M. Crocker, Catalytic deoxygenation of fatty acids and their derivatives to hydrocarbon fuels via decarboxylation/decarbonylation, J. Chem. Technol. Biotechnol. 87 (2012) 1041-1050.

[45] S. Mohapatra, T. Morgan, E. Santillan-Jimenez, M. Crocker, Conversion of Triglycerides and Fatty Acids to Hydrocarbons over Supported Nickel Catalysts, 22nd North American Catalysis Society Meeting, June 5-11, 2011, Detroit, Michigan.

[46] E. Santillan-Jimenez, T. Morgan, M. Crocker, Conversion of triglycerides and fatty acids to hydrocarbons via decarboxylation/decarbonylation (deCOx) over supported nickel catalysts, 7th International Conference on Environmental Catalysis, September 2-6, 2012, Lyon, France.

[47] J. Shoup, E. Santillan-Jimenez, T. Morgan, M. Crocker, Conversion of Triglycerides and Fatty Acids to Hydrocarbons Using Supported Nickel Catalysts, 2012 AIChE Annual Meeting, October 28 - November 2, 2012, Pittsburgh, Pennsylvania.

[48] V.A. Yakovlev, S.A. Khromova, O.V. Sherstyuk, V.O. Dundich, D.Y. Ermakov, V.M. Novopashina, M.Y. Lebedev, O. Bulavchenko, V.N. Parmon, Development of new catalytic systems for upgraded biofuels production from bio-crude-oil and biodiesel, Catal. Today 144 (2009) 362-366.

[49] E. Santillan-Jimenez, T. Morgan, J. Shoup, M. Crocker, Catalytic deoxygenation of triglycerides and fatty acids to hydrocarbons over Ni-Al layered double hydroxide, Energy & Fuels (2013), submitted.